Virginia Commonwealth University
VCU Scholars Compass

Theses and Dissertations | Graduate School

2005

Evidence for Absence of Latchbridge Formation in Phasic Saphenous Artery

Shaojie Han
Virginia Commonwealth University

Follow this and additional works at: https://scholarscompass.vcu.edu/etd

 Part of the Pediatrics Commons

© The Author

Downloaded from
https://scholarscompass.vcu.edu/etd/948

This Thesis is brought to you for free and open access by the Graduate School at VCU Scholars Compass. It has been accepted for inclusion in Theses and Dissertations by an authorized administrator of VCU Scholars Compass. For more information, please contact libcompass@vcu.edu.

www.manaraa.com

EVIDENCE FOR ABSENCE OF LATCHBRIDGE FORMATION IN PHASIC SAPHENOUS ARTERY

A thesis submitted in partial fulfillment of the requirements for the degree of Masters of Science at Virginia Commonwealth University.

by

SHAOJIE HAN
Masters of Medicine, Tongji Medical College, China, 2002
Bachelor of Medicine, Tongji Medical College, China, 1995

Director: PAUL H. RATZ, PH.D.
PROFESSOR, DEPARTMENT OF BIOCHEMISTRY AND PEDIATRICS

Virginia Commonwealth University
Richmond, Virginia
August 2005

Acknowledgement

I would like to thank my parents, Weizhong Han and Sue Xu, for always believing in me and supporting me. I would like to thank my wife Gan for always giving me directions when I get lost. I would like to thank Krystina Berg, Amy Miner, Tracey Webb, Dr. John Speich, Dr. Thomas Eddinger for their assistance and thoughtfulness with this project. I would like to thank the members of my committee for their support. I would like to thank Dr. George Ford for his help in my study. Last but not least I would like to thank Dr. Paul Ratz for providing the opportunity and direction to make this project and more possible.

Table of Contents

List of Figures

Page

List of Abbreviation

Full Name	Abbreviation
intracellular calcium	$[Ca^{2+}]_i$
8-bromo-guanosine 3',5'-cyclic monophosphate	8-Br-cGMP
Actin (thin filament)	A
Adenosin-5'-diphosphate	ADP
attached dephosphorylated cross bridge	AM
attached phosphorylated cross bridge	AMp
Analysis of variance	ANOVA
Antrum	Ant
Aorta	Ao
Adenosin 5'-triphosphate	ATP
Adenosin 5'-triphosphate disodium salt	$ATPNa_2$
Carotid artery	CA
Caldesmon	CalD
Calponin	CalP
Cytochalasin-D	cyto-D
Desmin	D
Detrusor smooth muscle	Det
Deep femoral artery	DF
Dimethyl Sulfoxide	DMSO
Dithiothreitol	DTT
Na_2 ethylenediamine tetraacetic acid	EDTA
ethylene glycol-bis(b-aminoethyl ether)-N,N,N',N'-tetraacetic acid	EGTA
Contractile force	F
Femoral artery	FA
Active force at optimal length	Fo
Fundus	Fun
G protein-coupled receptor	GPCR
Heat shock protein	HSP

inositol-1,4,5-trisphophate	InsP3
PSS in which 110 mM KCl was substituted isosmotically for NaCl	KPSS
Optimal length	Lo
Milli (10^{-3})	m
detached dephosphorylated cross bridge	M
Myosin light chain	MLC
17-kDa essential light chain of myosin	MLC17
myosin light chain kinase	MLCK
myosin light chain phoshatase	MLCP
morpholino-propanesulfonic acid	MOPS
detached phosphorylated cross bridge	Mp
myosin light chain phosphatase large regulatory subunit	MYPT1
Nano (10^{-9})	n
phenylephrine	PE
1,4-piperazin-bis-ethansulfonsaeure	PIPES
cyclic AMP-dependent kinase	PKA
cyclic GMP-dependent kinase	PKG
myosin light chain phosphatase catalytic subunit	PP1
physiological saline solution	PSS
physiological saline solution	PSS
Phentolamine	PT
Renal artery	RA
RhoA associated kinase	ROK
Saphenous artery	SA
Sodium Dodecyl Sulfate	SDS
Sodium Dodecyl Sulfate Polyacrylamide Gel Electrophoresis	SDS-PAGE
sarcoplasmic reticulum Ca^{2+} ATPase	SERCA
Smooth muscle myosin heavy chain isoform A	SMA
Smooth muscle myosin heavy chain isoform B	SMB
Tris Buffered Saline	TBS
Tropomyosin	Tm
Tween-Tris buffered Saline	TTBS
Micro (10^{-6})	u
Vimentin	V

Abstract

EVIDENCE FOR ABSENCE OF LATCHBRIDGE FORMATION IN PHASIC SAPHENOUS ARTERY

By Shaojie Han, B.M., M.M.

A thesis submitted in partial fulfillment of the requirements for the degree of Masters of Science at Virginia Commonwealth University.

Virginia Commonwealth University, 2005

Major Director: Paul H. Ratz Ph.D.
Professor, Department of Biochemistry and Pediatrics

Tonic arterial smooth muscle can produce strong contractions indefinitely by formation of slowly cycling crossbridges (latchbridges) that maintain force at a high energy economy. To fully understand the uniqueness of mechanisms regulating tonic arterial contraction, comparisons have been made to phasic visceral smooth muscles that do not sustain high forces. This study explored mechanisms of force maintenance in a phasic *artery* by comparing KCl-induced contractions in the tonic, femoral artery (FA) and its primary branch, the phasic saphenous artery (SA). KCl rapidly (<16 sec) caused strong increases in stress (1.2×10^5 N/m^2) and $[Ca^{2+}]_i$ (250 nM) in FA and SA. By 10 min, $[Ca^{2+}]_i$ declined to

175 nM in both tissues but stress was sustained in FA (1.3 x 10^5 N/m^2) and reduced by 40% in SA (0.8 x 10^5 N/m^2). Reduced tonic stress correlated with reduced myosin light chain (MLC) phosphorylation in SA (28% vs. 42% in FA). SA expressed more MLC phosphatase than FA, and permeabilized (β-escin) SA relaxed more rapidly than FA in the presence of MLC kinase blockade, suggesting that MLC phosphatase activity in SA was greater than that in FA. The reduction in MLC phosphorylation in SA was insufficient to account for reduced tonic force (latchbridge model), and SA expressed more "fast" myosin isoforms than did FA. Cytochalasin-D reduced force-maintenance more in FA than SA. These data support the hypothesis that strong force-maintenance is absent in SA because expressed motor proteins do not support latchbridge formation, and because actin polymerization is not stimulated.

CHAPTER 1 INTRODUCTION

1.1 smooth muscle force maintenance and the latch state

The smooth muscle cell of hollow organs must alter and set organ dimensions by contracting tonically against imposed loads. The economy of force maintenance is important for this purpose. Comparing to striated muscles, smooth muscles reveal striking differences in their economies of contraction. With less ATP consumption, the isometric contraction induced by 109mM K^+ can be maintained for at least 2 hours with little changes. Apparently, tonic smooth muscles benefit from this energy-saving contractile style, and play their biological role by maintaining tonic stress without fatigue. To explain this rather remarkable property of arterial smooth muscle, the latch bridge hypothesis, (slow detachment of dephosphorylated crossbridges) was proposed about 25 years ago. There are two phases that typically characterize the contractile response of tonic arterial smooth muscle to a stimulus such as KCl. The initial transients in cytosolic free Ca^{2+} ($[Ca^{2+}]_i$), myosin light chain (MLC) phosphorylation, crossbridge cycling rates are associated with rapid stress development. Then stress is maintained during the continued presence of the stimulus in the steady-state despite-reductions in $[Ca^{2+}]_i$, MLC

phosphorylation and crossbridge cycling rates and rate of ATP consumption. The steady-state phase was termed the latch state, which parallel the catch state in the muscles closing the shells of certain mollusks.

Force maintenance by tonic arterial muscle is attributed to the formation of latchbridges ((Dillon, Aksoy et al. 1981; Hai and Murphy 1988; Ratz, Hai et al. 1989) and reviewed by (Hai and Murphy 1989). A four-state kinetic model (Fig 1) was established by Hai and Murphy in 1988 to describe the latch bridge hypothesis.

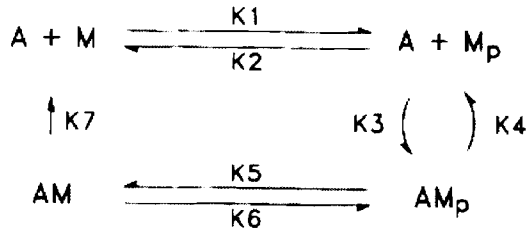

Figure 1. Structure of Hai-Murphy latchbridge model. A, Actin (thin filament); M, detached dephosphorylated cross bridge; Mp, detached phosphorylated cross bridge; AMp, attached phosphorylated cross bridge; AM, attached dephosphorylated cross bridge (latch bridge). *Hai, Murphy, Am. J. Physiol. 254:C99-C106, 1988*

The Hai-Murphy model depicted two types of crossbridge interactions: *1)* cycling phosphorylated cross bridges (A+Mp↔AMp) and *2)* noncycling dephosphorylated crossbridges (latch bridges, AM→A+M). The major assumptions are that *1)* Ca^{2+}-dependent myosin phosphorylation is the only postulated regulatory mechanism; *2)* each myosin head acts independently; *3)* latch bridges are formed by dephosphorylation of an attached cross bridge; *4)* AM→A+M is irreversible. Cross bridges cannot attach to the thin

filaments to form force-generating states unless they are first phosphorylated; *5)* All reactions exhibit first-order kinetics; *6)* Total myosin phosphorylation equals Mp+AMp and stress equals AM+AMp; *7)* The affinities of MLC Kinase (MLCK) and MLC phosphatase (MLCP) for detached and attached cross bridges are similar and set as $K_1=K_6$ and $K_2=K_5$; 8) the initial conditions for relaxed tissues are: [M]=1.0, [Ap]=[AMp]=[AM]=0, ($K_1=K_6=0$ corresponding to a $[Ca^{2+}]_I$ below the threshold for MLCK activation. Rates constants were resolved by fitting data on the time courses of myosin phosphorylation and stress development.

This kinetic model can be described by four differential equations:

$$d[M]/dt=-K_1[M]+K_2[Mp]+K_7[AM] \quad (1)$$

$$d[Mp]/dt=K_4[AMp]+K_1[M]-(K_2+K_3)[Mp] \quad (2)$$

$$d[AMp]/dt=K_3[Mp]+K_6[AM]-(K_4+K_5)[AMp] \quad (3)$$

$$d[AM]/dt=K_5[AMp]-(K_7+K_6)[AM] \quad (4)$$

A latchbridge has not been biochemically isolated for study, and the latchbridge model, although strongly supported (Rembold and Murphy 1990; Yu, Crago et al. 1997; Butler, Mooers et al. 1998; Mijailovich, Butler et al. 2000), is not universally accepted. (Butler, Siegman et al. 1986; Kenney, Hoar et al. 1990; Paul 1990). Butler and co-workers suggested that the cycling rate of given myosin head, regardless of its phosphorylation state, depends on the fraction of phosphorylated heads in the ensemble and is thus modulated as the extent of phosphorylation changes during a contraction.

However, recent kinetic biochemical studies support the concept of a high duty cycle for smooth muscle crossbridges (Khromov, Somlyo et al. 1995; Conibear 1999;

Gollub, Cremo et al. 1999; Baker, Brosseau et al. 2003). The Somlyos and their co-workers proposed that latch results from the prolonged attached lifetime of myosin binding with thin filament due to the high ADP affinity of minus-insert myosin (Fuglsang, Khromov et al. 1993). As the level of myosin phosphorylation declines with prolonged stimulation, the rate of cross bridge attachment is slowed significantly. Myosin dephosphorylation and the reduction in the cross bridge attachment rate results in a concomitant reduction in the ADP release rate, prolonging the force-bearing strong binding states, which will be mentioned again in Section 1.5.

1.2 Phasic and Tonic Smooth Muscles

The time-course, or profile, of an isometric smooth muscle contraction in response to KCl can be divided into an early, phasic portion reflecting the rapid increase in force to an initial high peak level upon initial muscle stimulation, and the steady-state, tonic portion during sustained stimulation reflecting the level of force that can be maintained by the muscle. Smooth muscles have been categorized as phasic or tonic, depending on the kinetics of force development, and whether the predominant KCl-induced force-profile reveals, respectively, a stronger phasic- than tonic-phase, or a tonic-phase that is at least equivalent to the strength of the peak contraction during the phasic phase (Somlyo and Somlyo 1968; Somlyo and Somlyo 1968). Smooth muscles belonging to the phasic group include most visceral muscles and the portal vein which contract rapidly and do not maintain force at high levels for long durations (Himpens, Matthijs et al. 1988). Tonic

smooth muscles are generally represented by arterial and airway smooth muscles (Horiuti, Somlyo et al. 1989).

Previous studies on regulatory mechanisms controlling tonic arterial and phasic visceral smooth muscle contractions suggested that at least elevated calcium levels, elevated MLC phosphorylation, or reduced crossbridge kinetics contribute to the tonic muscle force maintenance.

1.3 regulation of $[Ca^{2+}]_i$ in phasic and tonic smooth muscles

In the 1800 s, elevated $[Ca^{2+}]$i were considered as the primary regulator of muscle contraction (Reference: Ringer). More recent studies from Kathy Morgan's and Andrew Somlyo's laboratories, and others, showed using the photoprotein, aequorin and Ca^{2+} indicators, quin-2 and fura-2, that the resting $[Ca^{2+}]$i were 106±8 nM in tonic smooth muscle (rabbit pulmonary artery) and 79 ± 6 nM in phasic smooth muscle(ileum). In the phasic smooth muscle, the initial Ca^{2+} spike (374 ± 46 nM) was accompanied by an early force transient, maximum force, but in the tonic smooth muscle the initial Ca^{2+} spike (390 ± 34 nM) was accompanied by only about 48% of maximum force. After a transient peak, there was a decline to 70% of $[Ca^{2+}]$i peak value in tonic smooth muscle, and to 60% in phasic smooth muscle (Himpens and Somlyo 1988). Another example observed in a phasic muscle of canine antrum is a temporal change in Ca^{2+} sensitivity; Ca^{2+} sensitivity initially increases and then decreases during the spontaneous rhythmic contractions (Ozaki and Karaki 1993). In other words, $[Ca^{2+}]$i differences between phasic and tonic smooth muscle might determine their contractile characteristics.

Moreover, the sarcoplasmic reticulum also plays a major role in the regulation of Ca^{2+} in the smooth muscle. Structural and functional studies indicate the important role of the sarcoplasmic reticulum in excitation-contraction coupling in smooth muscles. As a source and sink of the Ca^{2+}, sarcoplasmic reticulum modulate the $[Ca^{2+}]i$ through inositol-1,4,5-triphosphate (InsP3) and ryanodine receptors and a Ca^{2+}-ATPase (SERCA) localized to its membranes. In smooth muscle Ca^{2+} is released mainly by stimuli that generate InsP3, which was distinguished from Ca^{2+}-induced Ca^{2+} release in striated muscle. Gene knockout mice have been reported for SR-associated protein, phospholamban, an inhibitor of SERCA2. Phospholamban can regulate both phasic and tonic smooth muscle contractility via modulation of SERCA(Paul, Shull et al. 2002). Gene-altered animal models have provided evidence clearly implicating the SR as a key modulator of smooth muscle Ca^{2+} and contractility, with the caveat that this modulation is tissue specific.

1.4 Ca^{2+} sensitization and desensitization: regulation of MLC phosphorylation ratio

It is generally accepted that Ca^{2+} sensitization and desensitization involve the major physiological mechanisms that regulate myosin activity: phosphorylation and dephosphorylation. Phosphorylation of MLC at Ser-19 permits myosin activation by actin, whereas dephosphorylation inactivates actin-activated myosin ATPase. G protein-coupled receptor (GPCR) agonists induce smooth muscle contraction by elevating $[Ca^{2+}]_i$ and by causing increased in Ca^{2+} sensitivity. Ca^{2+} sensitization can also be produced by high K+-induced contraction partly due to RhoA, RhoA associated kinase (ROK) and it's translocation resulting from the increase of $[Ca^{2+}]i$, (Urban, Berg et al. 2003). Thus, the

relative activity of the MLCK and MLCP is the major factor regulating the MLC phosphorylation and contraction (Somlyo and Somlyo 2003) (Fig 2).

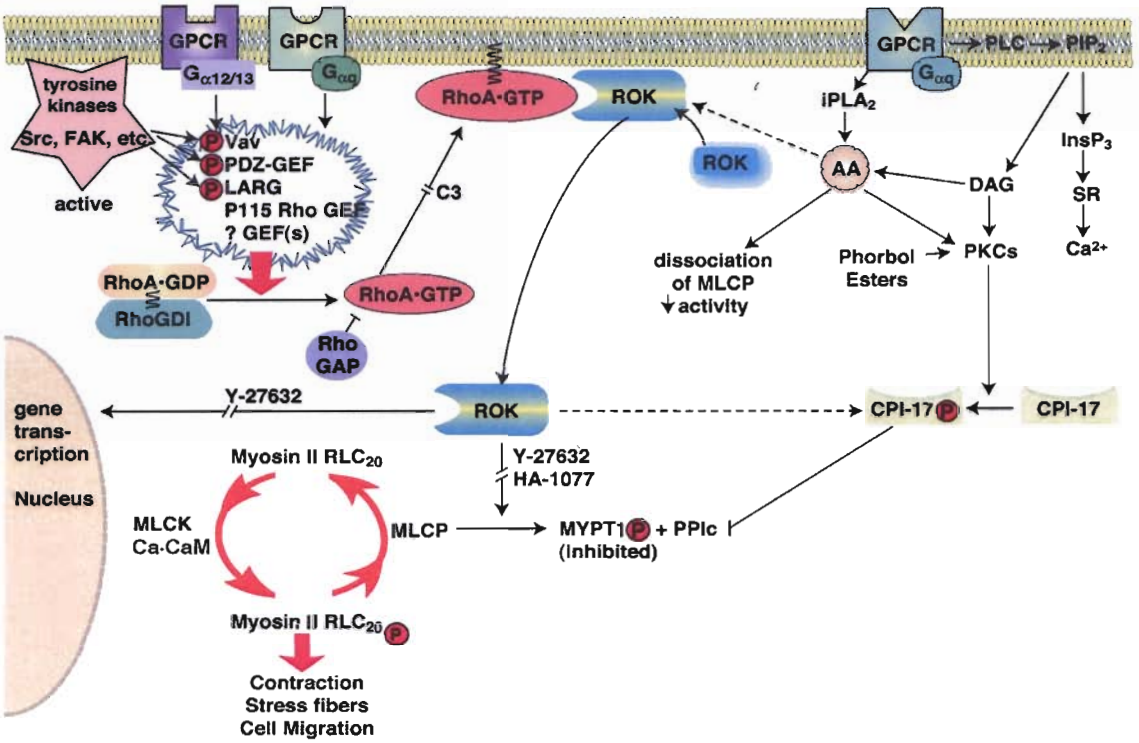

Figure 2. Signaling pathway for Ca^{2+} sensitization in smooth muscle. Activation GPCR initiates signaling through the cascades that inhibit MLCP, increase MLC phosphorylation and contraction. *Somlyo and Somlyo, Physiol Rev. 83: 1328-58, 2003*

It has been suggested that the Ca^{2+} sensitivity of force might differ between phasic and tonic smooth muscle (Gong, Cohen et al. 1992; Gong, Fuglsang et al. 1992). By studying β-Escin and α-toxin perimerablized femoral artery and ileum smooth muscle of guinea pig, Gong MC et al reported that tonic smooth muscle is more sensitive to the phosphatase inhibitors than phasic smooth muscle. The relaxation rate and

dephosphorylation rate are faster in phasic than tonic smooth muscle. MLCP and MLCK activities are 2.0- and 1.9-fold higher respectively in phasic than tonic smooth muscle. Since MLC phosphorylation turnover rate and phosphorylated MLC ratio largely, though not solely, depends on the enzyme kinetics and relative activity of MLCP and MLCK., the higher MLCP and MLCK activity, as well as the MLCP/MLCK constant rate might contribute to the lower steady state values of MLC phosphorylation and force in the phasic smooth muscle. What causes the differences in MLCP and MLCK activity between phasic and tonic smooth muscle, and especially between phasic and tonic *arterial* smooth muscle, remains to be fully understood.

Telokin, a 17-kDa acidic protein whose sequence is identical to the COOH terminus of MLCK, was proposed to induce Ca^{2+} desensitization. The expression of telokin is independently through a promoter located in intron of the MLCK gene. (Ito, Dabrowska et al. 1989) As a substrate of PKA and PKG, it is phosphorylated at Ser-13 in vivo, and it mediates 8-Br-cGMP induced smooth muscle relaxation by activating MLCP leading to the decrease of MLC phosphorylation. Studies show that telokin is highly expressed in visceral and venous smooth muscles which are phasic, compared with tonic femoral artery smooth muscle. The phasic ileum has 4.5 fold more telokin with two fold greater MLCP activity (Gong, Cohen et al. 1992) than the tonic femoral artery. However, the mechanism whereby telokin activates MLCP activity remains to be determined.

ROK activation, and PKC-dependent CPI-17 phosphorylation, lead to inhibition of MLC phosphatase and sustained MLC20 phosphorylation and contraction (Kitazawa, Eto et al. 2003; Huang, Zhou et al. 2005). Thiophosphorylated CPI-17 inhibits PP1c about

7,000-fold more efficiently than the nonphosphorylated form (Eto, Senba et al. 1997). The expression of CPI-17 and MYPT1 are tissue specific. It was found that vascular muscles contained more CPI-17 than visceral muscles, and phosphorylation of MYPT1 Thr(850) and CPI-17 Thr(38) contribute more to the inhibition of MLCP in vascular muscles than in visceral muscles. Moreover, the tonic femoral artery possessed approximately 8 times the cellular CPI-17 concentration of the phasic vas deferens. In contrast to CPI-17, phasic muscles contained more MYPT1 than tonic tissues (Woodsome, Eto et al. 2001). From the protein expression patterns, it is possible that CPI-17 and MYPT1 contribute to the regulation of the smooth muscle phasic and tonic contractile behavior.

1.5 Myosin Isoforms are responsible for crossbridge kinetics

In tonic, compared with phasic, smooth muscles the affinity of crossbridges is approximately 5 times higher for MgADP and the apparent second-order rate constant for MgATP is approximately 3 times lower (Fuglsang, Khromov et al. 1993), which could be the molecular basis of the 'latch'. Reduced crossbridge kinetics may be the result of differences in motor protein isoform expression (Rovner, Freyzon et al. 1997; Lauzon, Tyska et al. 1998; Szymanski, Chacko et al. 1998; Baker, Brosseau et al. 2003). Myosin is a member of a large family of motor proteins with a similar molecular structure, composed of two myosin heavy chains (MHCs) and two pairs of myosin light chains (MLCs). Smooth muscle expresses several different MHC and MLC isoforms: six MHC isoforms (four smooth muscle, two nonmuscle) and five MLC isoforms (two 17 kDa, two 20 kDa, one 23 kDa).

1.5.1 MLC17 isoforms

It was proposed that the isoforms of 17-kDa essential light chain of myosin (MLC17) is the major factor determining the MgADP affinity of myosin. Two MLC17 isoforms, acidic (MLC17a) and basic (MLC17b) isoforms, are products of a single gene generated by an alternative splicing mechanism, but differ in the substitution of five of the last nine amino acids at their carboxy termini. Phasic muscle was reported containing more MLC17a than MLC17b. Increasing myosin ATPase activity and faster movement are associated with MLC17a. Results from MLC17 isoforms exchange studies (Matthew, Khromov et al. 1998) show that the shortening velocity and rate of force development were approximately 1.5 and 2 times faster, respectively, in response to MLC17a than MLC17b in crossbriges with nonphosphorylated MLC, suggesting MLC17 isoforms contribute to the nucleotide affinity of latch bridges (Somlyo, Matthew et al. 1998).

1.5.2 Smooth muscle myosin heavy chain isoforms

Smooth muscle MHC isoforms result from the splicing of the single gene. Alternative splicing near the 3' end of the MHC pre-mRNA results in expression of either one of two proteins, SM1 (204 kDa) or SM2 (200 kDa), differing only at their carboxy termini. Although studies in permeabilized tissue strips show that SM1/SM2 isoforms related with ATPase activity and shortening velocity (Hewett, Martin et al. 1993), in vitro study on purified protein and single cells suggested these isoforms results in similar in vitro ATPase activities (Meer and Eddinger 1997).

Splicing at the 5' alternative splice site of the MHC gene results in two isoforms differing in the insertion (SMB) or omission (SMA) of 7- amino acids near the putative

ATP binding site. Expression of SMB is associated with a higher myosin ATPase activity, faster movement of actin filaments in in vitro motility assays (Kelley, Takahashi et al. 1993), and faster maximum shortening velocity (Eddinger and Meer 2001). Bladder from SMB KO mouse shorten slower than that from wildtype with SMB expression, consistent with SMB determining the shorten velocity of smooth muscle (Karagiannis, Babu et al. 2003).

1.5.3 Non-Muscle Myosin Heavy Chain

Tonic force maintenance has also been attributed to recruitment of non-muscle myosin (Morano, Chai et al. 2000; Lamounier-Zepter, Baltas et al. 2003) and reviewed by (Morano 2003)}. Nonmuscle-MHC can form thick filaments in smooth muscle cells of SM-MHC-deficient bladders. Nonmuscle myosin generated active force which was significantly lower and slower, and lacked an initial peak (Lofgren, Ekblad et al. 2003). It was suggest high ADP binding and low phosphate dependence of nonmuscle myosin would promote economical force maintenance of the cell.

Myosin isoforms and nonmuscle myosin might substantially influence the crossbridge kinetics. They could be the underlying molecular basis of latch. How they coexpress by tissue-specific pattern and how they determine the crossbridge kinetics, are still questions that need to be resolved.

1.6 Thin filament regulatory proteins and cytoskeletal alterations

An early hypothesis suggested that a filamin-actin-desmin domain participates in tonic force-maintenance (reviewed by (Rasmussen, Takuwa et al. 1987)}, and a recent

study using stiffness measurements suggests that a non-crossbridge component can participate in receptor agonist-induced maintenance of tonic contraction (Rhee and Brozovich 2003). There is compelling evidence that thin filament regulatory proteins participate in regulation of contraction (Marston, Pinter et al. 1992; Haeberle 1994; Obara, Szymanski et al. 1996; Earley, Su et al. 1998; Yan, Sen et al. 2003; Hai and Kim 2004), and although their principal action may be to maintain smooth muscle in the relaxed state ((Albrecht, Schneider et al. 1997; Malmqvist, Trybus et al. 1997; Lee, Gallant et al. 2000) and reviewed by (Trybus 1991)), there is evidence that thin filament regulatory proteins may also play a role in force-maintenance by cross-linking actin and myosin ((Sutherland and Walsh 1989; Walsh and Sutherland 1989) and reviewed by (Szymanski 2004)).

Tropomyosin (Tm), in striated muscle, provides the calcium switch for turning myosin ATPase activity on and off by interacting with troponin complex, but its function in smooth muscle is less clear because no troponin was found. However, some evidence shows that Tm has a cooperativity function in smooth muscle contraction. Binding of smooth muscle myosin and actin leads to the helpful movement of Tm, which is also facilitated by myosin phosphorylation.

Caldesmon (CalD) is an actin, Tm, myosin, and calmodulin binding protein. Its carboxy-terminal domains are responsible for inhibition of ATPase activity in vitro. Binding calmodulin or phosphorylation of sites between two actin-binding domain can reverse some of the inhibitory activity of CalD in vitro. In vivo studies from peptide antagonist approaches and antisense oligonucleotides suggests that, indeed, CalD is involved in suppressing smooth muscle tone.

Calponin (CalP) has amino acid sequences which shows high degree of structure homology to the inhibitory site of troponin-I. Binding with thin filament, CalP inhibits crossbridge cycling and acts as a load-bearing protein.

SM22 is an abundant, smooth muscle-specific, 22-kDa protein with unknown function. Whether or not SM22 serve as a functional thin filament regulatory protein is controversial. Although SM22-deficient mouse did not show obvious functional abnormalities in either visceral or vascular smooth muscle, changes in the thin filament distribution was observed, suggesting the possible role for SM22 in cytoskeletal organization.

Some of chaperon proteins, such as heat shock proteins (HSP20) and (HSP27) were also reported to modulate the myosin and actin interaction through thin filament regulatory mechanisms, when they are phosphorylated by signaling molecules(Bitar 2002; Meeks, Ripley et al. 2005).

Tonic force maintenance has also been attributed to cytoskeletal alterations involving changes in microfilament and microtubule polymerization (Wright and Hurn 1994; Battistella-Patterson, Wang et al. 1997; Mehta and Gunst 1999; Flavahan, Bailey et al. 2005).

The field of thin filament regulation of smooth muscle contractility is filled with controversy. However, these novel regulatory mechanisms provide new approaches to explain the latch bridges and steady-state force maintenance.

1.7 Objective

Regulation of phasic visceral smooth muscle appears to be considerably different than regulation of tonic arterial smooth muscle (Harnett, Cao et al. 2005)~~)~~. Also, rhoA kinase (ROK) plays a prominent role in regulation of the tonic-phase, but not the early phasic-phase of arterial contractions (reviewed by (Ratz, Berg et al. 2005)), but participates in both phasic- and tonic-phases of contraction in the phasic detrusor smooth muscle ((Ratz, Meehl et al. 2002) and figure 6 of this study). Moreover, although arterial smooth muscle is generally classified as tonic muscle, arterial smooth muscles from some vascular beds, such as mesenteric artery, are phasic, and the degree of phasic activity is more pronounced in smaller than larger arteries (Asano and Nomura 2003). What remains is to delineate the subcellular regulatory mechanisms directing an artery to contract in a tonic or phasic fashion.

The goal of this study was to identify the subcellular mechanisms causing tonic and phasic arterial smooth muscle contractions. We discovered that the rabbit saphenous artery (SA), a muscular branch of the tonic femoral artery (FA), contracts in a phasic manner. By studying tonic FA and phasic SA, we were able to use arterial smooth muscles from the same vascular bed to directly identify and compare the underlying mechanisms controlling phasic and tonic contractile behaviors.

CHAPTER 2 MATERIALS AND METHODS

2.1 Tissue Preparation

Tissues were prepared as previously described (Ratz 1993). New Zealand white rabbits (3-4 kg) were anesthetized and killed as approved by the Medical College of Virginia at Virginia Commonwealth University Institutional Animal Care and Use Committee protocol #0305-3208. Smooth muscle tissues were dissected and stored in cold (4C°) physiological saline solution (PSS; in mM: 140 NaCl, 4.7 KCl, 1.2 $MgSO_4$, 1.6 $CaCl_2$, 1.2 $NaHPO_4$, 2.0 MOPS adjusted to pH 7.4, 0.02 Na_2EDTA to chelate heavy metals, and 5.6 D-glucose). High-purity (17 MΩ) deionized water was used throughout the study. Fat and adventitia were removed mechanically under a binocular dissecting microscope (Olympus SZX12), and for all arteries, the endothelium was removed by gentle rubbing of the intimal surface with a rough metal rod approximately the size of the arterial lumen diameter. Arteries were cut with dissecting scissors into 2-3 mm-wide rings. Detrusor strips free of underlying urothelium were dissected from bladders from which the serosa was removed.

2.2 Isometric Force

Contractile force (F) was measured as previously described (Ratz 1993). Each muscle was mounted in a tissue bath in a Myograph System-610M (Danish Myo Technology, Denmark) between two stainless steel hooks, one of which was attached to a micrometer for length adjustments and the other to an isometric force transducer for force measurements. Voltage signals from the Myograph were digitized and visualized on a computer screen as F (in g). Data were acquired through an analog-digital converter board (National Instruments) and analyzed using DASYLab (DasyTech, Amherst, NH) and Microsoft Excel (Microsoft) software. Following equilibration for 1 hour at 37°C in aerated PSS, the muscle length for which active force was maximum (Lo) was determined for each tissue using an abbreviated length-tension curve and KPSS (PSS in which 110 mM KCl was substituted isosmotically for NaCl) as the stimulus (Herlihy and Murphy 1973; Ratz and Murphy 1987). In order to eliminate effects of norepinephrine released from periarterial nerve terminals, 1 μM phentolamine was used to block the α1-adrenergic receptors. To prevent acetylcholine-induced activation of detrusor strips upon KCl stimulation, 1 μM atropine was included in the bath solution. To measure muscle stress (F / cross-sectional area), at the end of the experiment, wet weight (mg) was recorded for each tissue, and muscle stress (S) in N/m^2 was calculated as (F (g) × 9.807×10^{-3} N / g) / ((wet wt (mg) / Lo (mm)) × 9.52×10^{-7} m^2·mm / mg).

2.3 Tissue Histology

To measure medial wall thickness and numbers of cell layers in the media, arterial rings were fixed in 2% glutaraldehyde in 0.1 M sodium cacodylate buffer overnight, washed with 0.1 M cacodylate buffer for 5-10 minutes, and then fixed by 1% osmium tetroxide in 1.0 M sodium cacodylate buffer for 1 hour at 4°C. Tissues were dehydrated by exposure to 50, 70, 80, and 90% ethanol for 5-10 min each followed by three changes of 100% ethanol for 10-20 minutes each at room temperature. Ethanol was replaced with 3, 10-20 minutes washes of 100% propylene oxide at room temperature before addition of a 1:1 mixture of PolyBed 812 resin and propylene oxide for at least 4 hours. Tissues were embeded in molds with PolyBed 812 resin, and the molds placed in an oven at 60-65°C for about 24-48 hours until resin polymerization was completed. Resin blocks were cut into 1 μ-thick sections with an ultramicrotome and transferred onto a drop of distilled water on a clean microscope slide. Sections were covered with 0.1% Toluidine blue / 0.1% methylene blue / 0.1% azure II in 1% sodium borate solution (Lynn, Martin et al. 1966) and heated on a hot plate for 3 minutes. Slides were rinsed in running water, returned to the hot plate to dry thoroughly, and a cover glass was affixed to each slide using a drop of Permount. Wall thickness of each artery was measured and the numbers of cell-layers for each cross-section was counted using a microscope (Olympus IX71) and OpenLab software (Improvision).

2.4 Measurements of 17 kDa MLC (MLC17) Isoform Expression and the Level of 20 kDa MLC (MLC20-p) Phosphorylation

Two-dimensional (isoelectric focusing / sodium dodecylsulfate) PAGE was performed as previously described (Ratz 1993; Urban, Berg et al. 2003) to measure the degree of MLC20-p and the fractional expression of MLC17a and MLC17b isoforms. Arteries at Lo were quick-frozen in an acetone-dry ice slurry, warmed slowly to room temperature, dried, weighed, and homogenized in 8 M urea, 2% Triton X-100, and 20 mM dithiothreitol. Isoelectric variants of MLCs were separated by isoelectric focusing using an ampholyte range of 4.5-5.4, and after proteins were separated according to molecular weight, they were transferred to Immobilon membranes (Millipore Co. Bedford, MA) by electrophoresis, then visualized using colloidal gold total protein stain (Bio-Rad Lab, Hercules, CA). The relative amounts of phosphorylated MLC20-p and of MLC17a and MLC17b were quantified by digital image analysis (Scion Image, NIH) and calculated using the respective formulas: MLC20-p = MLC20-p / (MLC20-p + unphosphorylated MLC20), and MLC17a = MLC17a / (MLC17a + MLC17b).

2.5 Western immunoblotting for expression analysis of MLCP and rhoA kinase α (ROKα)

Expression levels of MLCP catalytic subunit 1-δ (PP1 δ), MLCP regulatory subunit, MYPT1, and a regulator of MLCP activity, ROKα, were measured by sodium dodecylsulfate (SDS)-PAGE and Western blot. Arteries at Lo were frozen, dried and weighed as described above, then homogenized in a 1-D sample buffer solution (~400 μl buffer / mg tissue) containing 25 mM Tris-HCl (pH 6.8), 10% glycerol, 20 mM DTT, 5 mM EGTA, 1 mM EDTA, 50 mM NaF, 1 mM Na_3VO_4, 0.005% bromophenol blue, 1%

SDS, and the protease inhibitors, Leupeptin, Aprotinin and APMSF at 20 μg / ml each. Proteins were separated by SDS-PAGE using 7.5% polyacrylamide for MYPT1 and ROKα, and 12% polyacrylamide for PP1 δ, followed by transfer onto Immobilon membranes. Protein loading was verified to be constant across all lanes by MEMCode (Pierce) staining. Immobilon membranes were blocked with 5% non-fat milk in Tris-buffered saline containing 0.05% (w/v) Tween-20 for 1 hour and then incubated with primary antibodies overnight at 4°C. The following dilutions of primary antibodies were used: anti-PP1δ at 1:500 (Upstate), anti-MYPT1 at 1:500 (BD Transduction Laboratories), and anti-ROKα at 1:200 (Santa Cruz Biotechnology). Horseradish peroxidase-conjugated goat polyclonal antibody was used as secondary antibody and the amounts of specific protein were detected by enhanced chemiluminescence (Amersham). Protein bands were quantified after digitization by Scion Image Software.

2.6 PAGE and Western immunoblotting for myosin heavy chain (MHC) isoform expression analysis

Rabbit tissues for protein analysis were homogenized in sample buffer containing 0.125 M Tris, 2% sodium dodecylsulfate (wt/vol), 20% glycerol, 0.1% bromophenol blue (wt/vol) and 20 mM dithiothreitol. MHCs were resolved on low cross-linking sodium dodecylsulfate gels using the method of Giulian and colleagues (Giulian, Moss et al. 1983), and immunoblotting was performed as previously described (Eddinger and Wolf 1993). Polyclonal antibodies to the SMB (plus 7 amino acid head insert isoform) and SMA (minus 7 amino acid head insert) smooth muscle MHC isoforms were generated in rabbits

using the following peptides (SMA polypeptide - 'N'--KKDTSITGELEC--'C'; SMB polypeptide -"N"-- QGPSLAYGELEC--'C"). Antiserum was tested on ELISA against expressed SMA and SMB sub-fragment 1 polypeptides. Both antibodies were shown to have at least 100 fold higher affinity for their appropriate antigen than for the alternative isoforms. Smooth muscle and non-muscle MHC specific antisera were obtained from Biomedical Technologies (Stoughton, MA). Western immunoblots were reacted as reported previously (Gaylinn, Eddinger et al. 1989).

2.7 2D proteome

Tissues were homogenized in Rehydration Buffer (Urea 7 M, Thiourea 2 M, 0.2% Triton X-100, Immobilized pH Gradient (IPG) buffer 0.5%, Bromophenol Blue 0.002%, Na2ethylenediamine tetraacetic acid 1 mM, APMSF 20ug/ml, Aprotonin 20ug/ml, Leupeptin 20ug/ml, DTT 2.8mg/ml) on ice. Isoelectrical focusing was run on IPG strips (pH 4-7, 11cm) in a Bio-Rad Protean IEF Cell, and proteins were separated by SDS-PAGE on 4-20% Criterion Tris-HCl Gels (Bio-Rad). Proteins were identified by staining with SYPRO Ruby (BioRad) and digital images (Molecular Imager FX, Bio-Rad) were analyzed using PDQuest image analysis software (Bio-Rad).

2.8 $[Ca^{2+}]_i$

$[Ca^{2+}]i$ was measured as previously described (Ratz 1993) with minor modifications. Tissues at Lo in an aerated muscle chamber designed for microscopic imaging (Danish Myo Technology, Denmark) placed on the stage of an inverted

microscope (Olympus IX71) were loaded for 2.5 hours with 7.5 μM fura 2-PE3 (AM) and 0.01% (wt/vol) Pluronic F-127 (TefLabs, Austin, TX) to enhance solubility. After 3, 10 min bath changes with PSS to remove extracellular fura, the fluorescence emission at 510 nm was collected by a photomultiplier tube for excitations at 340 nm and 380 nm (DeltaRam V, Photon Technologies Inc., Lawrenceville, NJ) and emission intensities were expressed as 340 nm / 380 nm ratios using Felix software (Photon Technology International) to measure changes in $[Ca^{2+}]i$. At the end of the experiment, minimum (R_{min}) and maximum (R_{max}) fluorescence ratios were obtained by treating tissues with, respectively, a Ca^{2+}-free KPSS containing 5 mM EGTA and 30 μM ionomycin, and a high calcium (3.2 mM Ca^{2+}) KPSS containing 30 μM ionomycin. Background fluorescence, determined by incubating tissues in 4 mM MnCl2 plus 30 μM ionomycin, was subtracted from all 340 nm and 380 nm signals prior to calculating the 340 nm / 380nm fluorescence ratios. Intracellular Ca^{2+} concentrations were calculated as described by (Grynkiewicz, Poenie et al. 1985) using the following formula: $[Ca^{2+}]i = K_d (S_f/S_b) [(R-R_{min})/(R_{max}-R)]$, where K_d (Ca^{2+}/fura dissociation constant) was estimated as 224 nM. R was the experimentally determined ratio of fluorescence intensities at 340 and 380 nm corrected for the background fluorescence at each wavelength, and S_f and S_b values were obtained from background-subtracted fluorescence intensity values measured during excitation at 380 nm during the R_{min} and R_{max} protocols, respectively.

2.9 Tissue permeabilization

Artery rings at Lo were depleted of sarcoplasmic reticular Ca^{2+} by contracting 3-times with 10 μM phenylephrine in a Ca^{2+}-free solution. Tissues were then permeabilized at 5° C for 45 minutes with β-escin (40 μM for FA and 100 μM for SA; the higher concentration for SA was used because of its thicker media), and continued for 60 minutes at 30° C. The initial treatment with β-escin at a low temperature helps the slow penetration and/or binding of β-escin to the surface membrane of the smooth muscle cells (Masuo, Reardon et al. 1994). β-escin was dissolved in a "relaxing solution" contained 74.1 mM potassium methanesulphonate, 4.0 mM magnesium methanesulphonate, 4 mM Na_2ATP, 4 mM EGTA, 5 mM creatine phosphate, 4 mM EGTA and 30 mM PIPES, neutralized with 1 M KOH to pH 7.1 at 20° C. Ionic strength was kept constant at 0.18 M by adjusting the concentration of potassium methanesulfonate. To activate muscle contraction at Ca^{2+}-clamped levels of 1 μM (pCa = 6) free Ca^{2+}, a "contracting solution" was made by including the appropriate volume of a 1 M $CaCl_2$ stock (Fluka Chemicals) as determined using WEBMAXC (Patton, Thompson et al. 2004). Calmodulin (1 μM) was added to the solutions throughout each experiment to compensate for its loss during permeabilization. To induce relaxation for relaxation velocity measurements, tissues pre-contracted by pCa = 6 contracting solution were rapidly washed in the relaxing solution (pCa = 9) that included 3 μM wortmannin to inhibit MLC kinase activity. During relaxation, one set of tissues was frozen and MLC phosphorylation was measured.

2.10 Latchbridge model simulation

The Hai-Murphy kinetic 4-state latchbridge model was simulated using MATLab 6.5 with Simulink 5.0 (The MathWorks, Inc.) using the same initial conditions and assumptions as those used by Hai and Murphy (Hai and Murphy 1988). Because MATLAB 6.5 permits the use of time-varying constants, this feature was employed for rate constants simulating changes in MLC kinase and phosphatase activities to more closely reflect the time-varying changes in $[Ca^{2+}]i$ (and thus, MLC kinase activity), and regulation of MLCP by ROK (reviewed by (Ratz, Berg et al. 2005)).

2.11 Drugs

Receptor antagonists used to prevent endogenous receptor activation due to neurotransmitter release upon KCl-stimulation of tissues were, for arteries, 1 μM phentolamine, and for detrusor, 1 μM atropine. β-escin was used to permeabilize tissues, and calmodulin was added to replace that lost by permeabilization. All of the above were from Sigma (St. Louis, MO). Wortmannin, Y-27632, cytochalasin-D and ionomycin were from Calbiochem (La Jolla, CA). β-escin was dissolved in DMSO for a stock concentration of 10 mM. Cytochalasin-D and ionomycin were dissolved in 100% ethanol for stock solutions of 10 mM. Vehicles (DMSO and ethanol) were added to control tissues at no more than 0.1%, which had no effect on contractions. All other drugs were dissolved in distilled water.

2.12 Statistics

The null hypothesis was examined using Students' t-test (when 2 groups were compared) or using a one-way analysis of variance (ANOVA). To determine differences between groups following ANOVA, the Student-Neuman-Keuls post-hoc test was used. In all cases, the null hypothesis was rejected at $P<0.05$. For each study described, the n value was equal to the number of rabbits from which arteries were taken. Statistical analyses and curve fitting were performed using Prism 3.02 (GraphPad Software, Inc., San Diego, CA).

CHAPTER 3 RESULTS

3.1 Structure

Of the two major branch arteries that bifurcate from the femoral artery (FA) just cranial to the knee, only the deep femoral (DF) both grossly (Fig 3Aa) and histologically (Figs 3Ab-3Ad) represented an extension of the FA, while the saphenous artery (SA) was structurally different than the FA (Fig 3Ab = DF; Fig 3Ac = FA; Fig 3Ad = SA). For example, FA and DF had equivalent medial thicknesses (Fig 3B) and numbers of cell layers within the media (Fig 3C) and nearly equivalent optimum lengths for muscle contraction (L_o; Fig 3D), a muscle mechanical measurement that reflects artery lumen diameter. However, compared to FA, SA media was ~2-fold thicker (Fig 3B) because of ~2-fold more medial cell layers (Fig 3C), but displayed a shorter L_o by ~ ½ (Fig 3D) correlating with a smaller zero-load lumen diameter (data not shown).

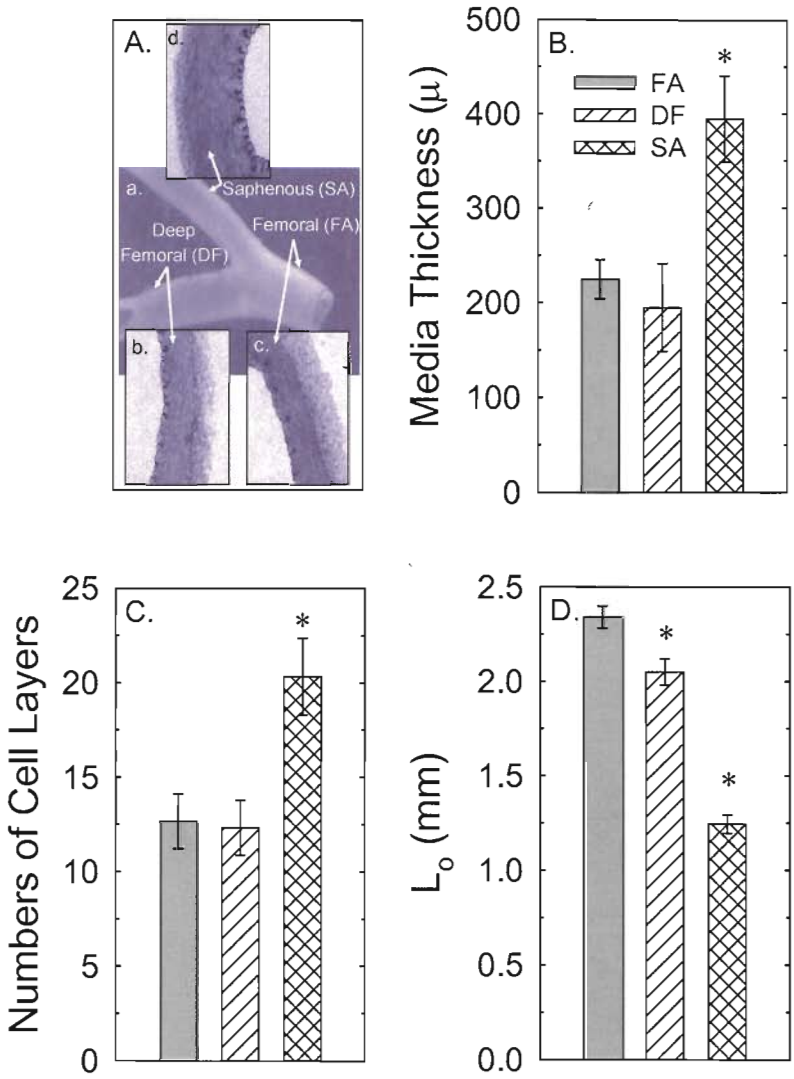

Figure 3. Gross (Aa) and fine (Ab-Ad) structures of rabbit femoral (FA; Aa & Ac), deep femoral (DF; Aa & Ab) and saphenous (SA; Aa & Ad) arteries. DF and SA bifurcate from the FA. FA and DF displayed the same medial thickness (B) and numbers of cell layers within the media (C) and nearly equivalent optimum lengths for muscle contraction (L_o, D), a muscle mechanical measurement that reflects lumen diameter. SA was ~2-fold thicker because of ~2-fold more medial cell layers, but displayed a shorter L_o correlating with a smaller lumen diameter. Data in B-D are means ± SE. $n = 3$, except Lo, where $n = 13$. * = $P < 0.05$ compared to FA.

3.2 Stress, $[Ca^{2+}]_i$ and MLC phosphorylation

KCl produced a tonic contraction in the FA and DF with equivalent time-dependent force values (Fig 4A & 4B), but produced a phasic contraction in the SA (Fig 4A). The peak stress value produced by SA was equal to the maximum tonic stress produced by the FA (Fig 3A). Stresses produced by the SA were reduced from the peak values by 5 and 10 min to a value ~60% that produced by the FA (Fig 4A). A maximum phenylephrine concentration (10 μM), like KCl, also produced tonic and phasic contractions in, respectively, FA and SA (data not shown). Despite divergent temporal changes in stress, FA and SA produced equivalent temporal changes in $[Ca^{2+}]_i$ when stimulated with KCl (Figs 4C & 4D). Thus, the difference in steady-state stress between FA and SA could not be ascribed to a reduction in $[Ca^{2+}]_i$.

KCl produced a rapid increase in the degree of MLC phosphorylation from a basal value of ~5% to ~40% within 4 sec in both FA and SA (Fig 5A). However, MLC phosphorylation continued to increase to over 60% by 10 sec in FA, but remained at ~40% in SA, a value statistically lower than that produced by FA (Fig 5A). MLC phosphorylation declined in both FA and SA to lower steady-state values. However, SA reached a steady-state MLC phosphorylation value of ~28% within 30 sec and remained at that level for at least 10 min, while FA produced a more gradual decline to a steady-state value at 10 min of ~42% (Fig 5A). The correlation in MLC phosphorylation and stress values (Fig 5B) suggest that the phasic nature of the KCl-induced contraction produced in SA was caused by the reduced level of steady-state MLC phosphorylation in SA compared to FA.

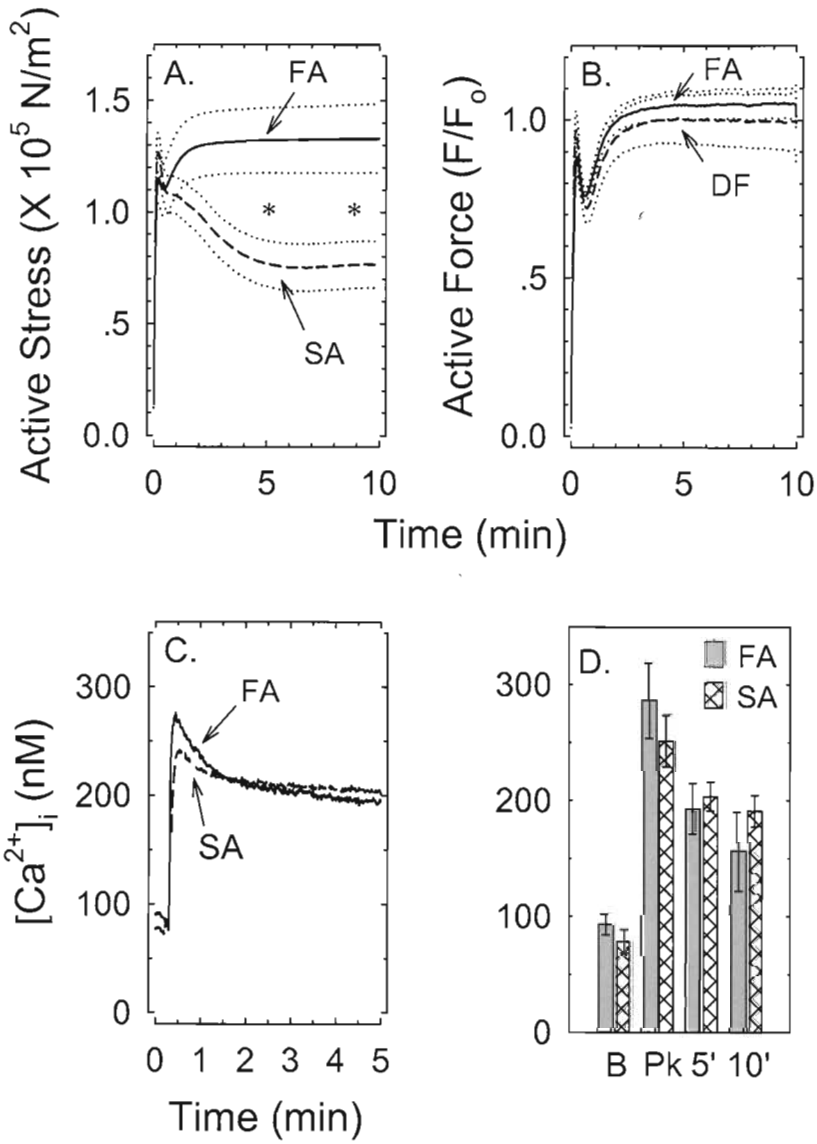

Figure 4. Force and $[Ca^{2+}]_i$ in KCl-stimulated Femoral (FA) and saphenous (SA) arteries. FA and SA produced equivalent early (16.2 ± 1.2 sec) peak increases in stress upon stimulation with KCl (~1.2 x 10^5 N/m^2) that remained at high levels for at least 10 min in FA but declined by 5 min in SA to ~0.8 x 10^5 N/m^2 (A). FA and deep femoral (DF) artery, and FA and SA, produced identical time-dependent KCl-induced profiles in, respectively, force (B) and $[Ca^{2+}]_i$ (C & D). "B" and "Pk" in panel D are, respectively, Basal and peak. Data are means (solid and dashed lines A-C and bars, D) ± SE (dotted lines in A & B). For clarity, SE values were removed from the curves in C and included in D. B: n = 10; C: n = 3; D: n = 6. * = $P < 0.05$ compared to FA.

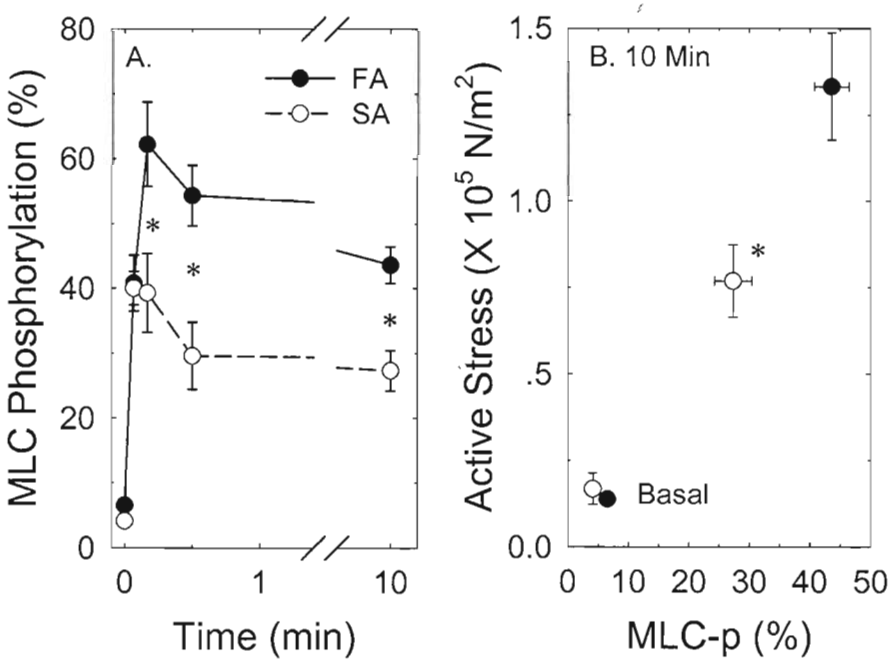

Figure 5. Basal (time = 0) and KCl-induced temporal increases in MLC phosphorylation (A) and the relationship between active stress and MLC phosphorylation (B) in femoral artery (FA) and saphenous artery (SA). Data are means ± SE. For phosphorylation data, *n* = 4-10.. = $P < 0.05$ compared to FA. Stress data is replotted from Fig 4.

3.3 Estimate of MLCP activity and expression of MLCP

The rate of relaxation of permeabilized arterial smooth muscle is limited by the rate of MLCP activity (Mitsui, Kitazawa et al. 1994). Thus, the rate of relaxation from a pre-contracted state induced by exposure of permeabilized tissues to a Ca^{2+}-free solution containing a MLC kinase inhibitor can be used as an indirect measure of the MLCP activity in Ca^{2+}-clamped but otherwise intact smooth muscle tissue (Lee, Li et al. 1997). Our data showed that SA produced a much more rapid relaxation compared to FA when tissues precontracted at pCa = 6 were exposed to a relaxing solution (containing EGTA, see "Methods") and the MLC kinase inhibitor, wortmannin (Fig 6A). The half-time for relaxation was nearly 2 min in FA, but less than 1 min in SA (Fig 6B). To ensure that relaxation rates reflected rates of MLC dephosphorylation in both FA and SA, MLC phosphorylation and force were measured simultaneously in one set of tissues. The nearly linear relationship between MLC phosphorylation and force (Fig 6C & 6D) supports the conclusion that relaxation rates in permeabilized tissues can be a surrogate measure of MLC dephosphorylation, and reflect MLCP activity (Mitsui, Kitazawa et al. 1994; Lee, Li et al. 1997). These data suggest that the lower MLC phosphorylation levels produced in intact (not permeabilized) SA compared to FA during a KCl-induced contraction are caused by a higher intrinsic MLCP activity in SA compared to FA.

We compared, in FA and SA, expressed levels of MLCP catalytic (PP1δ) and large regulatory (MYPT1) subunits, and ROK, an enzyme that plays a key role in the regulation of MLCP activity in KCl-induced tonic contractions (reviewed by (Ratz, Berg et al. 2005). SA expressed nearly 2-fold more PP1δ and ~1.3-fold more MYPT1 than did FA, but both

arteries expressed equal levels of ROK (Fig 7). These data suggest that one possible cause for increased MLCP activity in SA compared to FA is that SA expresses more MLCP such that the overall MLCP-to-kinase activity ratio is higher in SA.

3.4 Effects of Wortmannin and Y-27632

To determine whether MLC kinase and ROK-dependent MLCP play similar or different roles in SA and FA, intact tissues were contracted in the presence of the MLC kinase inhibitor, wortmannin, and the ROK inhibitor, Y-27632. Wortmannin produced identical inhibitions of both peak (Fig 8A) and steady-state (Fig 8B) contractions in SA and FA. Y-27632 likewise inhibited steady-state contractions in SA and FA with equal potency (Fig 8D), and had no effect on the peak contractile response produced by SA and FA (Fig 8C). In support of our previous finding (Ratz, Meehl et al. 2002), Y-27632 inhibited both peak and steady-state contractions of the phasic bladder smooth muscle (Figs 8C & 8D, triangles). These data suggest that additional regulatory systems other than MLC kinase and ROK-dependent MLCP are not required to explain KCl-induced steady-state (tonic-phase) contractions of SA and FA.

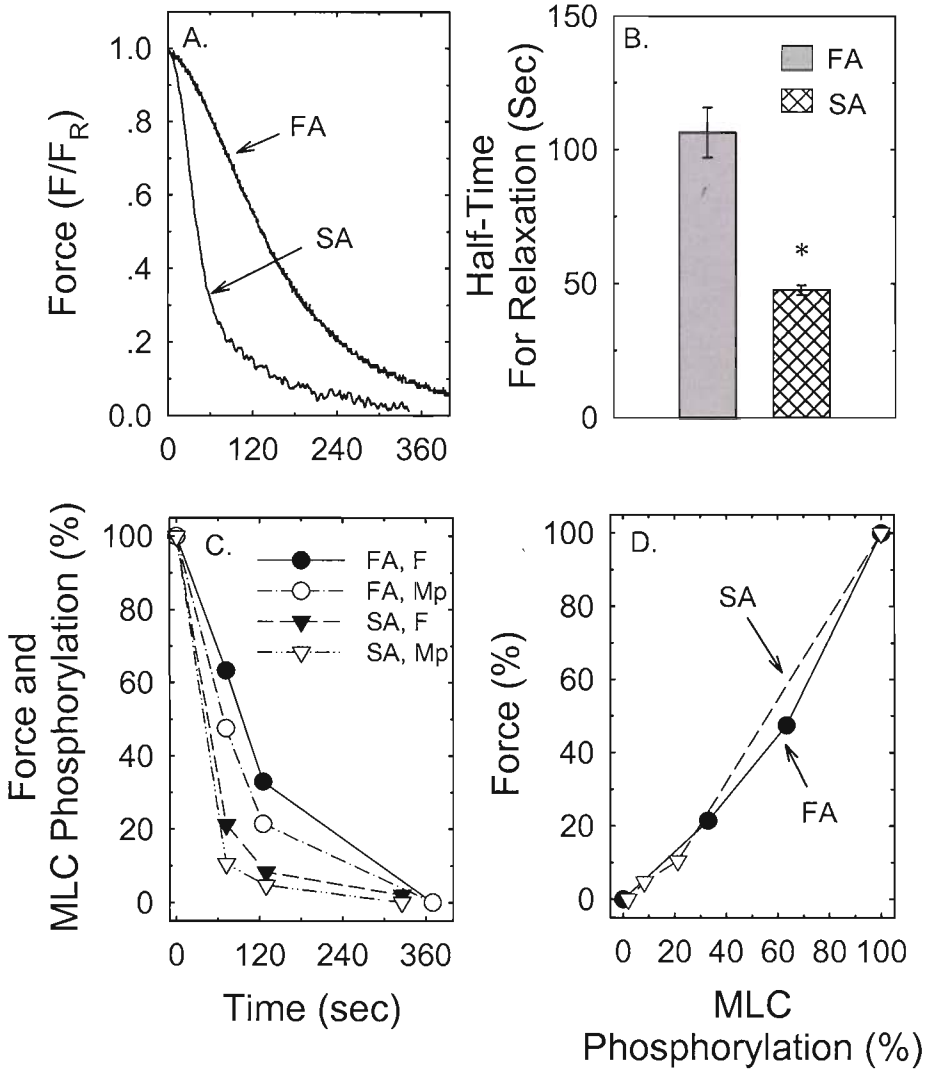

Figure 6. Time-dependent relaxation (A & C) and reduction in MLC phosphorylation (C), half-time for relaxation (B), and relationship between force and MLC phosphorylation produced during relaxation in β-escin-permeabilized rings of femoral artery (FA) and saphenous artery (SA). "F" and "Mp" in panel C are, respectively, force and MLC phosphorylation. Data in A are an example of a force tracing. Data in C & D are from one artery (n = 1). Data in B are means ± SE. n =4.. = $P < 0.05$ compared to FA.

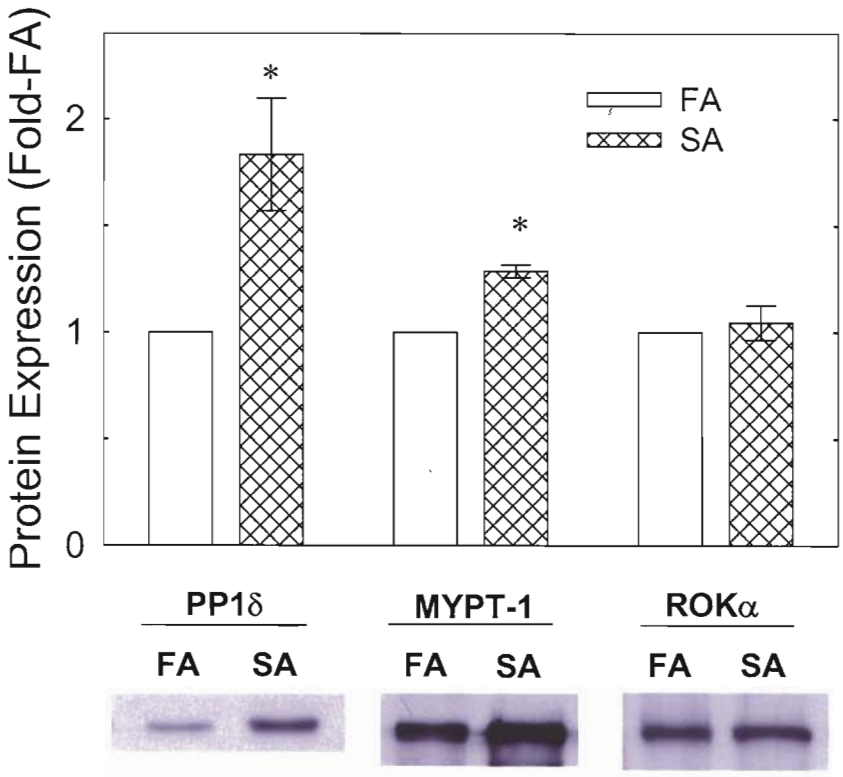

Figure 7. A comparison of expression of PP1δ, MYPT1 and ROKα in femoral artery (FA) and saphenous artery (SA). PP1δ = catalytic subunit of protein phosphatase -1 (MLCP is a PP1δ subtype), MYPT1 = myosin phosphatase targeting subunit-1, the large molecular weight regulatory subunit of MLCP, ROKα = rhoA kinase, a negative regulator of MLCP. Gel lanes were loaded with 20 μg (for PP1δ), 10 μg (for MYPT1) and 50 μg (for ROKα). Data for SA are means ± SE. $n = 6$. * = $P < 0.05$ compared to FA.

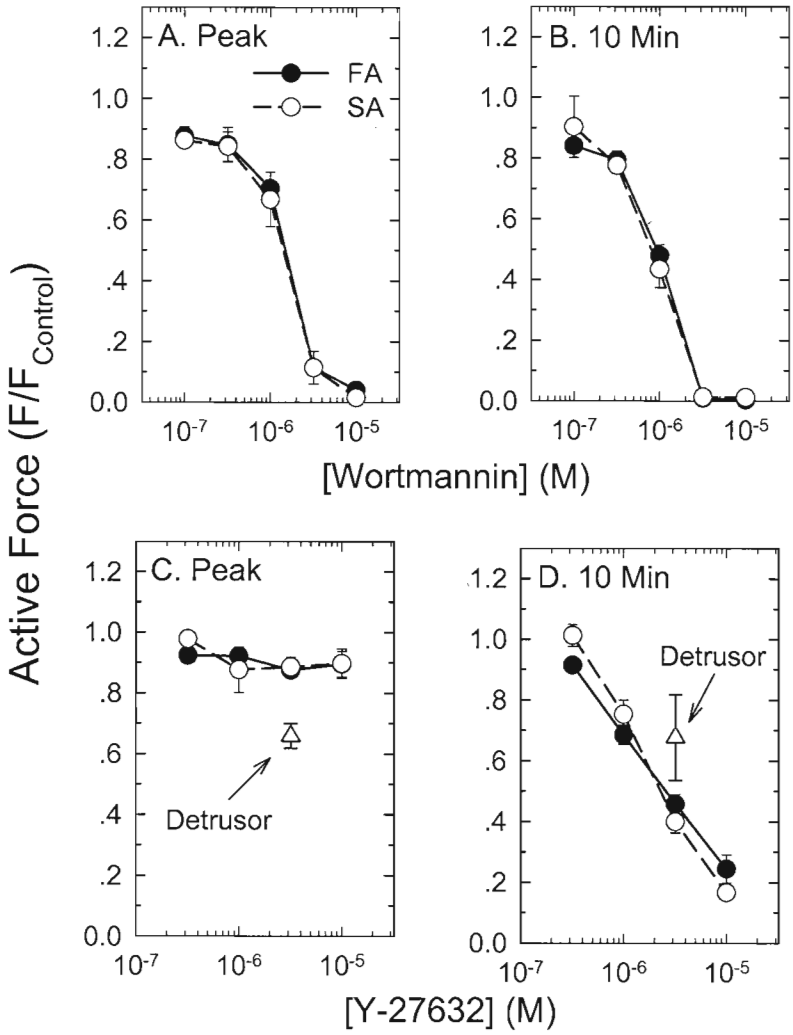

Figure 8. Effect of wortmannin (MLC kinase inhibitor) and Y-27632 (ROK inhibitor) on KCl-induced early peak (A & C) and tonic (10 min; B & D) force in femoral artery (FA) and saphenous artery (SA). For a comparison, the effect of Y-27632 on bladder wall (detrusor) smooth muscle was included (triangles, C & D). Data are means ± SE. n = 3-5.

3.5 Latchbridge model

The Hai-Murphy 4-state kinetic latchbridge model was employed to determine whether the reduction in KCl-induced steady-state MLC phosphorylation in SA compared to FA was sufficient to explain the phasic contractile behavior of SA. We used modeling rate constants (in s^{-1}) that were very similar to those used by Hai and Murphy to predict the behavior of the tonic swine carotid artery (Hai and Murphy 1988). However, rather than stepping k_1 & k_6 values from 0 to 0.55 for 5 sec and then down to 0.30 for the remainder of the simulated stimulation period to mimic changes in MLC kinase activity due to changes in $[Ca^{2+}]_i$ (Hai and Murphy 1988), we used similar values but modeled a more gradual change to more closely follow the change in $[Ca^{2+}]_i$ measured in SA and FA (Figs 9C & 9D). We also modeled a small temporal change in k_2 & k_5 values to reflect recent data (Ratz, Berg et al. 2005) indicating that KCl can activate ROK and produce a transient small increase in MYPT1 phosphorylation that may transiently reduce MLCP activity (Figs 9E and 7F). Using a k_4 value of 0.05, a k_3 value of 0.4, and, as in the original Hai-Murphy model (Hai and Murphy 1988), a k_7 (latchbridge) value $1/10^{th}$ that of the k_4 value ($k_7 = 0.005$), the modeled temporal change in MLC phosphorylation fit closely the empirically-derived MLC phosphorylation data for FA (Fig 9G). Our data showing that steady-state MLC phosphorylation (see Fig 6), but not $[Ca^{2+}]_i$ (see Fig 4D), was less in SA than FA suggested that MLCP in SA was greater than that in FA. Thus, k_2 & k_5 values used to model FA behavior were doubled to model SA behavior (Fig 9F). The resulting modeled change in MLC phosphorylation fairly closely matched the empirical MLC phosphorylation data for SA (Fig 9H).

The force response predicted based on a latchbridge-to-phosphorylated crossbridge detachment ratio (k_7 / k_4) of 0.1 very closely matched our empirical data for FA (Fig 9A, Model L_{FA}), but was a poor match for SA (Fig 9B, Model L_{SA}). When the detachment rate for a latchbridge was made to equal the detachment rate for a phosphorylated crossbridge (i.e., $k_7 / k_4 = 1$), the modeled force profile more closely fit the actual empirical data for SA (Fig 9B, Model NL_{SA}).

Because of the steeply hyperbolic dependency of steady-state force on steady-state MLC phosphorylation in tonic arterial smooth muscle (Ratz, Hai et al. 1989), and because force "saturates" at modest levels of MLC phosphorylation (Ratz, Hai et al. 1989; Ratz 1993), a reduction in MLC phosphorylation from over 40% to just under 30% will not necessarily result in a significant reduction in force. Rather, total force will remain relatively constant as the fraction of phosphorylated, attached crossbridges (AMp) is reduced and the fraction of unphosphorylated, attached crossbridges (AM, latchbridges) is proportionally increased (Fig 10B). That is, the modeled force profiles for FA and SA were found to be nearly equivalent despite large differences in MLC phosphorylation values because the proportion of crossbridges contributing to steady-state (5 min) force for the FA was ~60% AM (latchbridge) and ~40% AMp (phosphorylated, attached crossbridge), whereas that for SA was ~73% AM and ~27% AMp (Fig 10B). Thus, the reason why a reduction in the level of MLC phosphorylation from ~42% to ~28% did not cause a comparable reduction in force in the 4-state kinetic simulation has a straightforward and readily predictable explanation based on the Hai-Murphy latchbridge model. Elimination

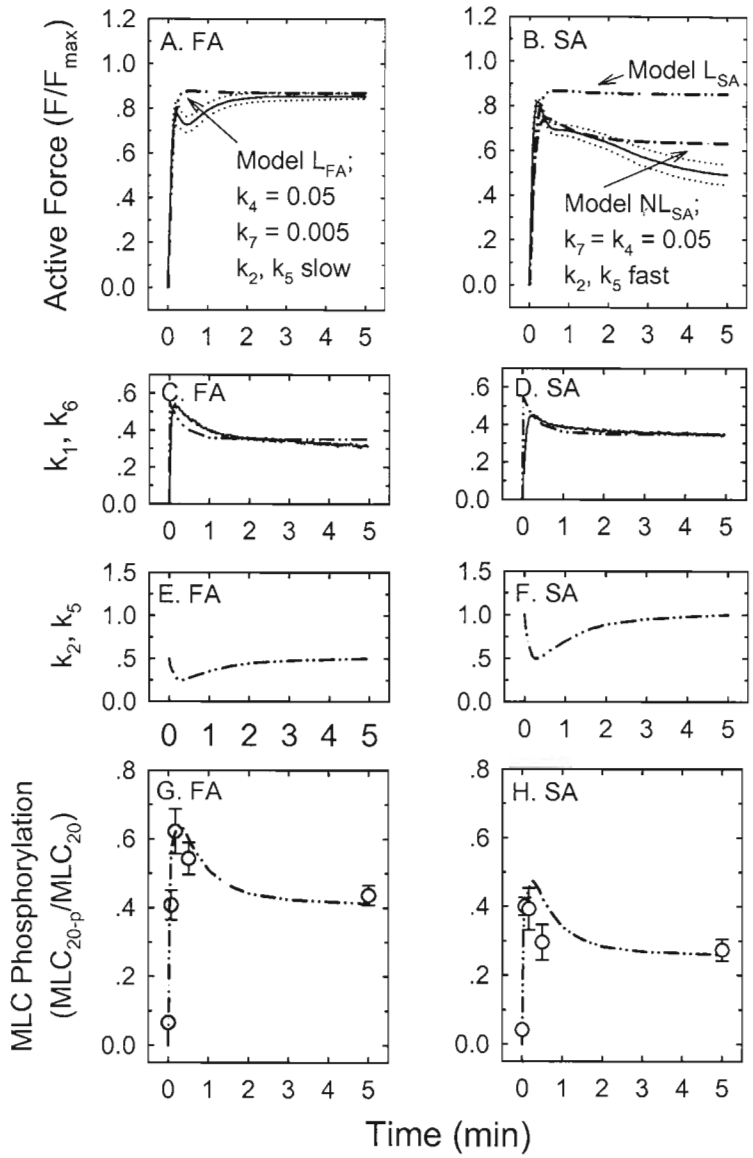

Figure 9. Hai-Murphy 4-state kinetic latchbridge model simulation (dash-dot lines) and empirical data (solid lines and open symbols) for femoral artery (FA) and saphenous artery (SA). L_{FA} (A) and L_{SA} (B) equal simulations where k_7 = 0.1-fold k_4 (i.e., k_7 refers to the very slow detachment rate of a latchbridge) for, respectively, FA and SA. NL_{SA} (B) equals a simulation for SA where $k_7 = k_4 = 0.05$ (i.e., the rate of detachment of AM = rate of detachment of AMp, and thus, reflects the absence of a latchbridge state). Empirical data for C & D are normalized Ca^{2+} tracings derived from Fig 4C. Empirical MLC phosphorylation data are from Fig 5A.

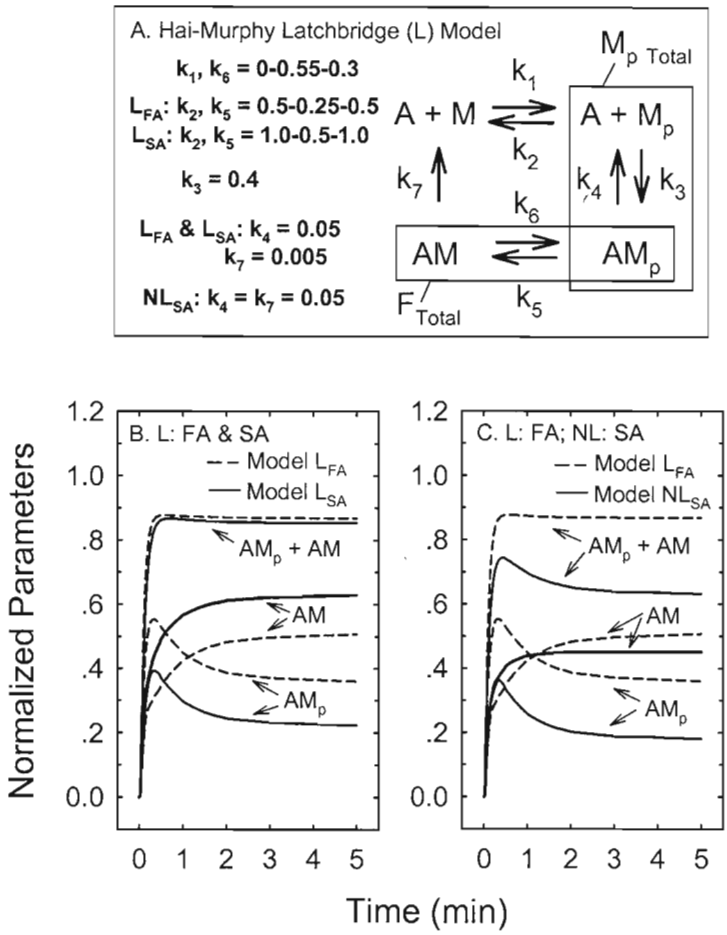

Figure 10. Hai-Murphy 4-state kinetic latchbridge model (A, right side) and kinetic constants (A, left side) used for the simulation displayed in Fig 9 and in panels B & C of this figure. A = actin, M = myosin, Mp = MLC phosphorylated species where myosin is in the unattached state, AMp = MLC phosphorylated species where myosin is in the actin-attached (crossbridge) state, AM = dephosphorylated, attached crossbridges that can bear a load (latchbridges). Total force = AM + AMp. Total MLC phosphorylation = Mp + AMp. L_{FA}, L_{SA} refer to model simulations where k_7 = 0.1-fold k_4 (latchbridge is included) for both femoral artery (FA) and saphenous artery (SA). NL_{SA} refers to a model simulation where $k_7 = k_4$ (no latchbridge is included). Note that model simulations designed to provide steady-state Mp values > 20% permit strong force maintenance because of latchbridge formation (B). Compared to the relatively low level of latchbridge species formed (B, dashed line, AM) at a relatively high level of simulated Mp (B, dashed line, AMp) mimicking empirical data from the tonic, FA, a lower level of simulated Mp (B, solid line, AMp) that mimics the level found to occur in the phasic SA yields a *higher* level of the latchbridge species (B, solid line, AM). Thus, despite a lower level of MLC

phosphorylation in SA, latchbridge formation would disallow phasic contractile behavior (AMp + AM = force). Absence of the latchbridge state (C, NL_{SA}, $k_7 = k_4$) in the simulation permits a more phasic contraction (C, solid line compared to dashed line, AMp + AM) that more closely mimics the empirical temporal force profile produced in SA upon KCl-induced stimulation.

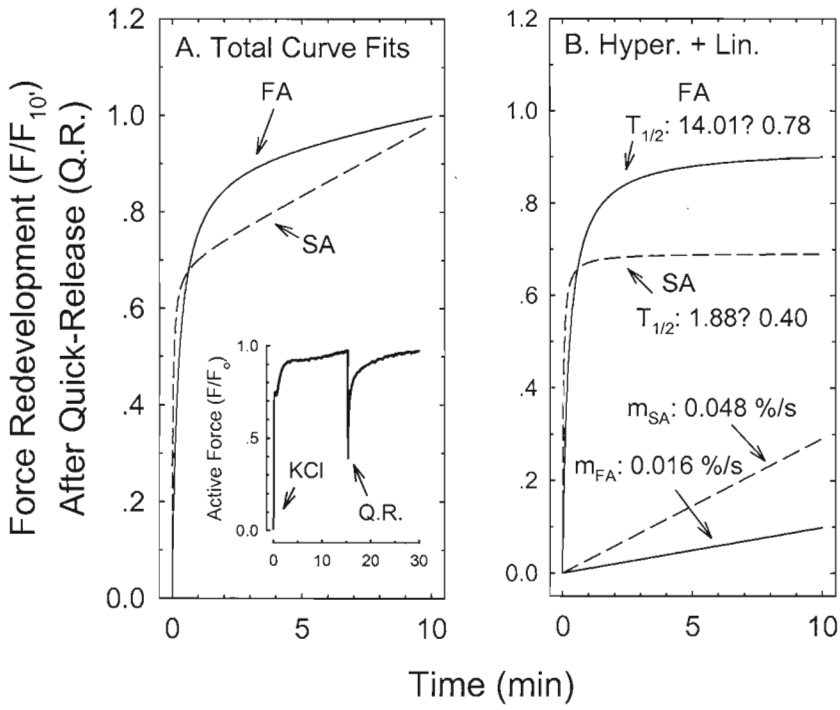

Figure 11. A hyperbolic + linear curve provides a good modeling fit ($r^2 > 0.97$) for force redevelopment following a quick step-decrease in muscle length of 10% (quick release, Q.R., inset of panel A) during the steady-state of a KCl-induced contraction for both femoral artery (FA) and saphenous artery (SA). Half-lives ($T_{1/2}$) and slopes (m) of the curves for FA and SA and the individual hyperbolic and linear portions of the curves are shown in panel B. $n = 4$.

of the latchbridge (without eliminating the myosin species, AM) by making k4 and k7 equal (no latch; NLSA, Fig 10) caused force to become phasic as apposed to tonic because of a reduction in the amount of AM present in SA compared to FA (Fig 10C).

3.6 Rates of force redevelopment upon quick-release

Steady-state levels of MLC phosphorylation correlate with steady-state levels of the velocity of muscle shortening (Ratz, Hai et al. 1989), and the rate of force redevelopment upon quick-release (Q.R., Fig 11A) is a measure of the velocity of muscle shortening (Dillon and Murphy 1982). The proposed reason for a correlation between MLC phosphorylation levels and the rate of force redevelopment is that the cycling crossbridge-to-latchbridge ratio (AMp / AM) is higher at higher levels of MLC phosphorylation (see Fig 10). Thus, if SA contains latchbridges, then SA should re-contract more slowly than FA upon quick-release at ~10 min of contraction because SA produced significantly lower MLC phosphorylation levels at this time (see Fig 5). Our empirical data revealed the opposite. Namely, that the rate of force redevelopment produced by SA was signficantly higher than that for FA (Fig 11). Using a curve fitting program (GraphPad Prism), the rate of force redevelopment for both arteries produced a good fit (r^2 = 0.996 for FA, 0.974 for SA) to an equation consisting of one fast hyperbolic and one slower linear component (Fig 11A). The half-time ($T_{½}$) for force redevelopment for the hyperbolic component of FA was over 7-fold longer than that for SA (i.e., the rate of force redevelopment for SA was over 7-fold faster than FA; Fig 11B), and the slope of the slower, linear component for SA (m_{SA}) was 3-fold faster than for FA (m_{FA}; Fig 11B).

These data together support the hypothesis that FA does, but SA does not, form latchbridges to maintain high levels of steady-state force.

3.7 Smooth muscle motor protein expression levels

Higher rates of force redevelopment for SA compared to FA support the hypothesis that SA contains "faster" motor protein isoforms than FA ((Arner, Lofgren et al. 2003) for review). To test this hypothesis, the relative expression of 17 kDa essential myosin light chain (MLC_{17}) isoforms, $MLC17_a$ and $MLC17_b$, were examined using 2-D PAGE, and smooth muscle myosin heavy chain (MHC) isoforms that do (SMB) and do not (SMA) contain a 7 amino acid insert were examined using Western Blot and selective antibodies. Tonic muscles, defined as those smooth muscles that produce sustained, high levels of steady-state force, and phasic muscles, defined as those smooth muscles that produce initial high levels of force that decline to much lower steady-state values, were investigated. The tonic FA, DF and renal artery (RA) displayed ~50-60% MLC_{17a}, whereas the phasic SA and detrusor (Det) displayed 90-100% MLC_{17a} (Fig 12a). Tonic aorta (Ao), carotid artery (CA), FA, RA and stomach fundus (Fun) displayed higher relative expression levels of SMA compared to SMB, whereas phasic SA and stomach antrum (Ant) displayed higher relative levels of SMB compared to SMA (Figs 12Bd & 12Be). None of the smooth muscles examined expressed enough non-muscle myosin to be detected when compared to an equal protein loading of platelets that express non-muscle rather than smooth muscle myosin (Fig 12Bc). These data support the notion that SA produced faster force redevelopment than FA despite lower MLC phosphorylation levels at

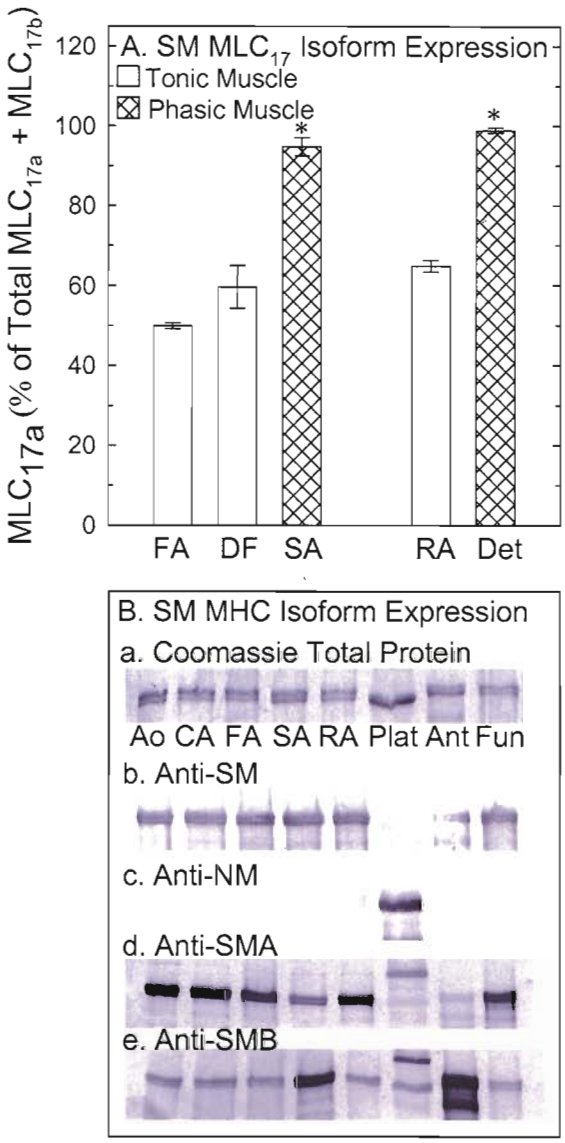

Figure 12. Essential myosin light chain (MLC_{17}) isoform expression levels for the tonic femoral artery (FA), deep femoral artery (DF) and renal artery (RA) compared to the phasic saphenous artery (SA) and detrusor (Det; A). Panel B displays total protein (Ba) and relative levels of myosin (Bb), non-muscle myosin (Bc), and smooth muscle myosin heavy chain (SM MHC) expression for the "slow" SMA isoform (Bd) and "fast" SMA isoform (Be) for tonic aorta (Ao), carotid artery (CA), FA, RA and stomach fundus (Fun) compared to the phasic SA and stomach antrum (Ant). Plat = rabbit platelet. Data in panel A are means ± SE, n = 4-5.. = $P < 0.05$. Data for panel B is an example derived from an $n = 3$.

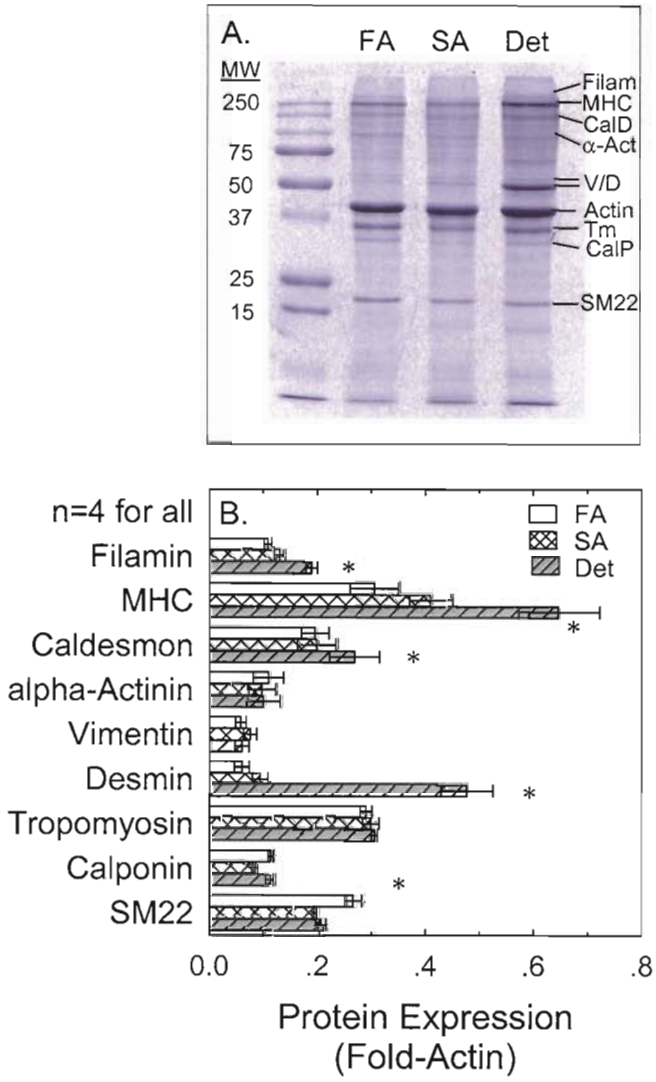

Figure 13. Comparison of proteins expressed in a high abundance by tonic and phasic arteries (respectively, femoral, FA, and saphenous, SA, arteries), and phasic visceral smooth muscle (detrusor; Det). Proteins identified with Coomassie blue stain are filamin (Filam), myosin heavy chain (MHC), caldesmon (CalD), α-actinin (α -Act), vimentin (V), desmin (D), actin (Actin), tropomyosin (Tm), calponin (CalP) and SM22. A: Example of a stained gel; all lanes were loaded with 10 μg protein. B: quantification of bands normalized in-lane to actin. Data are means ± SE. $n = 4$.* = $P < 0.05$ compared to FA.

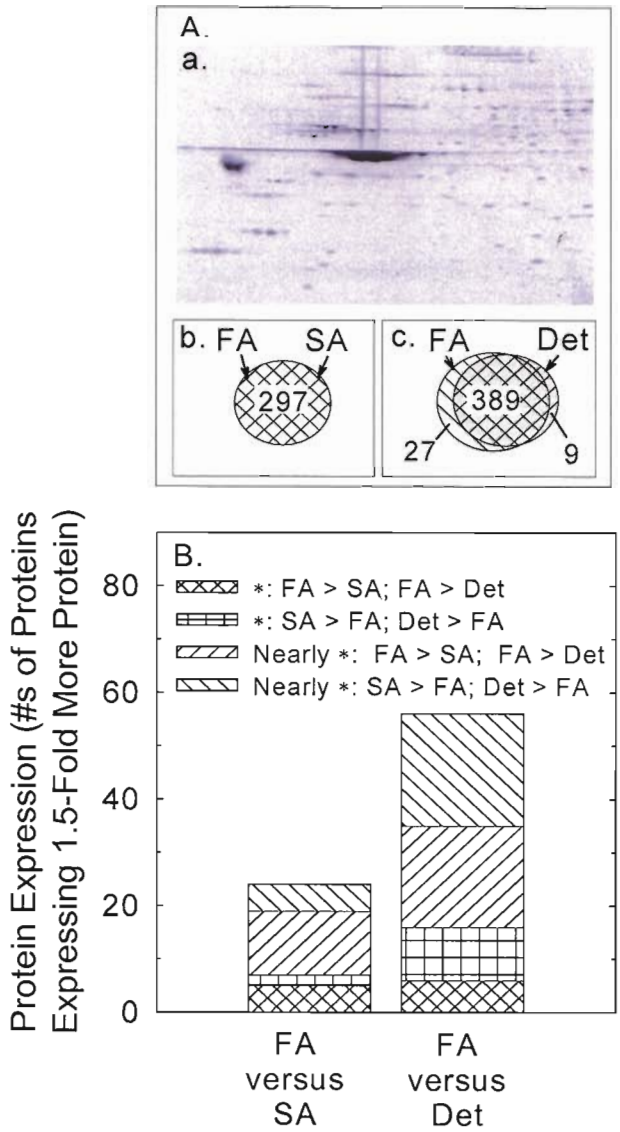

Figure 14. Comparison of the smooth muscle proteome, limited to a pI range of 4-7 and a molecular weight range of 6.4-200 kDa, for femoral artery (FA), saphenous artery (SA) and detrusor (Det). Aa: example of a SYPRO ruby-stained 2-D gel of SA. Ab & Ac: Venn diagrams (not to scale) showing that all proteins identified in the comparisons between FA and SA could be found in both groups (b), but that of the 389 proteins found when comparing FA to Det, 27 were only found in FA but not in Det, and 9 were found only in Det and not in FA (c). B: quantification of proteins found in common but that were expressed by one smooth muscle at 1.5-fold greater or lesser levels compared to the other smooth muscle.. = statistically different. Nearly. = average values for protein expression levels were 1.5-fold different, but the difference was not statistically significant presumably because of the low n value. $n = 3$.

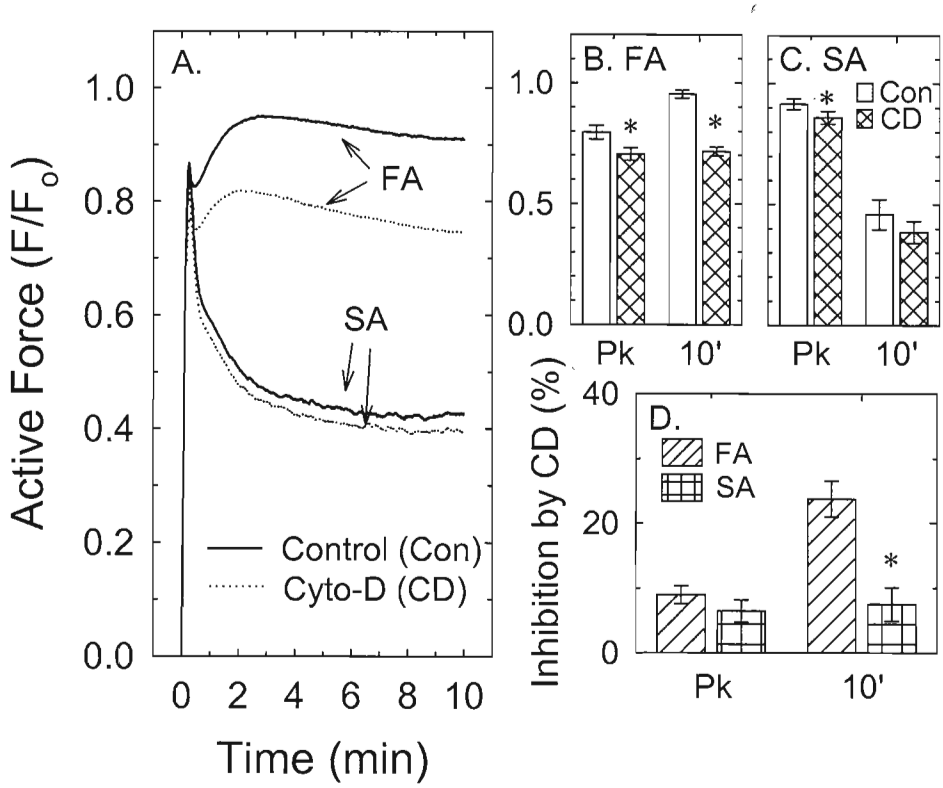

Figure 15. Effect of an inhibitor of actin polymerization, cytochalasin-D (cyto-D; CD), on the strength of the overall contractions (A), and specifically, on the early phasic (Pk) and tonic (10) portions of contractions (B-D), produced by KCl in femoral artery (FA) and saphenous artery (SA). The percent difference between control (Con) and cyto-D-treated tissues is shown in panel D. Data are means ± SE. n = 4., = $P < 0.05$ compared to control (B & C) and compared to FA (D).

steady-state because SA expressed quantitatively more "faster" (SMB and MLC_{17a}) compared to "slower" (SMA and MLC_{17b}) myosin isoforms ((Arner, Lofgren et al. 2003).

3.8 Proteomic analysis

Based on its temporal contractile profile and motor protein isoform composition, the SA may be categorized along with detrusor and stomach antrum as a phasic smooth muscle. Thus, the contractile phenotype and the motor protein genotype of SA are more similar to that of a visceral smooth muscle than to its "parent" tonic arterial smooth muscle, the FA. Regulation of smooth muscle contraction requires the interaction of many complex signaling, metabolic and structural systems, and whether some arterial muscles are more closely related overall to visceral smooth muscles or to each other is an important question that remains to be determined. To determine whether the overall protein expression profile of SA is more like that of a phasic visceral smooth muscle or a tonic arterial smooth muscle, an initial proteomic analysis was performed.

The abundance of highly-expressed proteins relative to actin in FA, SA and detrusor were compared using 1-D PAGE (Fig 13A). Of the 9 abundantly expressed proteins readily identified by Coomassie blue staining that likely participate in contraction (Weber, Seto et al. 2000), 4, filamin, MHC, caldesmon (CalD) and desmin, were expressed in greater, and 1, calponin (CalP), was expressed in lesser abundance in the phasic, detrusor compared to tonic FA. None of the 9 proteins displayed differential expression when comparing SA to FA (Fig 13B).

A more comprehensive analysis was performed using 2-D PAGE and PDQuest software to compare protein expression within a pI range of 4-7 and a molecular weight range of 6.4-200 kDa (Fig 14Aa). All of the 297 proteins identified on 6 gels from an $n = 3$ of FA were also identified on 6 gels from an $n = 3$ of SA (Fig 14Ab). Of 389 proteins identified on 6 gels from an $n = 3$ of FA and on 6 gels from an $n = 3$ of Det, 27 proteins were expressed by FA but not by detrusor, and 9 proteins were expressed by detrusor and not by FA (Fig 14Ab). In addition, of the proteins expressed in common, the levels of expressed proteins were more different when comparing FA and Det than when comparing FA and SA (Fig 14B). In particular, ~15 proteins displayed more than a 1.5-fold difference in level of expression when comparing FA and Det whereas only 6 proteins displayed a 1.5-fold difference in level of expression when comparing FA and SA (Fig 14, cross-hatched and checkered bars). When including proteins that displayed a trend for a 1.5-fold difference in expression (numbers were nearly significantly different, hatched bars in Fig 14B), there were nearly 60 proteins with high expression-level differences when comparing FA and Det, but only ~25 proteins displaying differences in expression levels when comparing FA and SA. These data suggest that based on commonality of expressed proteins, FA and SA are more genotypically similar than FA and Det.

3.9 Effect of cytochalasin-D

To test the hypothesis that the tonic-phase of arterial contractions are maintained by increases in actin polymerization, FA and SA were contracted in the presence of cytochalasin-D, an agent that binds to the barbed-end of actin to inhibit polymerization

(reviewed by (Cooper 1987)). Exposure of tissues to 0.2 μM Cytochalasin-D for 15 min prior to stimulation with KCl, and during the KCl-induced contraction, caused a small (~5-10%) inhibition in the early peak force in both FA (Pk, Figs 15B & 15D) and SA (Pk, Figs 15C & 15D), and a small (~5-10%) reduction in the average tonic force in SA that was not statistically different (10 , Figs 15C & 15D). Cytochalasin-D produced a larger, ~20% reduction in tonic force produced by KCl in FA (10 , Figs 15B & 15D). These data suggest that actin polymerization contributes to tonic force maintenance in FA but not SA.

CHAPTER 4 DISCUSSION

Results from the present study support the hypothesis that differential motor protein isoform expression and actin polymerization determine whether arterial smooth muscle produces a transient (phasic) or sustained (tonic) isometric contraction. Our data suggest that latchbridges were formed only by FA and not SA, and that the determining factor for latchbridge formation was expression of "slower" myosin isoforms. SA expressed only the "faster" myosin isoforms, did not display enhanced actin polymerization during a KCl-induced contraction, as did FA, and did not maintain high levels of stress. Thus, we propose that the absence of both latchbridge formation and enhanced actin polymerization in the phasic SA precluded its ability to maintain high levels of force for the duration of a KCl-induced stimulation period. However, differential regulation of other proteins, such as thin-filament regulatory proteins, can not at this time be ruled out as playing a role in controlling force maintenance. Although our data clearly demonstrate that actin polymerization was enhanced during the steady-state of a KCl-induced contraction in FA and not SA, the mechanism causing this differential regulation of actin polymerization remains to be determined.

The concept that actin polymerization plays an important role in regulation of contraction has been described for airway smooth muscle, another tonic muscle (reviewed by (Gerthoffer and Gunst 2001)), and very recently, for the myogenic contraction of arterioles, a tonic contraction produced in response to increases in transmural pressure (Flavahan, Bailey et al. 2005). Wright and colleagues, using rat aorta (Wright and Hurn 1994; Battistella-Patterson, Wang et al. 1997), demonstrated that the entire tonic- phase, but not the early phasic-phase, of a KCl-induced contraction was dependent on actin polymerization. We found that the early phasic phase of contraction in both FA and SA was inhibited ~10% by cytochalasin-D when used at 0.2 μM, but that the tonic portion of a contraction produced in FA, but not SA, was inhibited more than 20%. What distinguishes our model from that described by Wright and colleagues, is that our model includes both increased actin polymerization and latchbridges as playing important roles in force maintenance in tonic arterial muscle because actin polymerization does not appear to account entirely for tonic force maintenance, at least in the rabbit FA. Precisely how enhanced actin polymerization permitted enhanced stress-maintenance was not determined, but because force redeveloped upon quick-release, crossbridge cycling appeared to remain the primary (perhaps sole) force generator.

A hallmark of tonic smooth muscle is an ability to contract to high stress levels indefinitely without fatiguing (Murphy 1988; Murphy 1994). This characteristic would seem crucial for the normal physiological function of arterial smooth muscle, which must

contract against high pressures, sometimes for very long durations. Most visceral smooth muscles, with the exception of sphincters and the stomach fundus, can produce high levels of stress only transiently, and isometric contractions of these muscles is therefore characterized as phasic. The subcellular mechanisms responsible for causing tonic versus phasic smooth muscle contractile behavior have been a matter of considerable debate, in part, because comparisons have been made between tonic arterial muscles and phasic visceral muscles. Regulation of visceral smooth muscles can be significantly different than regulation of tonic arterial smooth muscles (reviewed by (Harnett, Cao et al. 2005)). We confirmed this notion by showing that, whereas the phasic portion of a KCl-induced contraction produced by SA and FA were not affected by the ROK inhibitor, Y-27632, both phasic and tonic force components produced by detrusor were inhibited equally well by Y-27632 (see Fig 6). Also, our preliminary proteomic analysis comparing visceral detrusor with arterial muscle revealed that detrusor and FA were genotypically more different than SA and FA. To our knowledge, the present study is the 1st to directly compare arterial segments that exist anatomically adjacent to one another within the same vascular tree, that are of comparable size, contract to identical levels of stress and that clearly display tonic versus phasic contractile behavior. This comparison enabled us to determine that, unlike the tonic FA, the phasic SA did not appear to enter the latch-state.

The latch-state is characterized by maintenance of high force levels in the face of falling indices of muscle activation, including $[Ca^{2+}]_i$, MLC phosphorylation and the maximum rate of crossbridge cycling. Although $[Ca^{2+}]_i$ and MLC phosphorylation fell to

low levels after initially reaching high levels early (within ~16 sec) upon muscle stimulation by KCl, stress produced by SA likewise fell ~40% compared to the tonic FA. As anticipated, a computer simulation based on the latchbridge model demonstrated that the reductions in MLC phosphorylation by 5 and 10 min from the early, high, peak values did not predict a fall in stress in FA or SA. Rather, the latchbridge model predicted that the temporal stress profile should have been maintained at nearly the same level in SA and FA even though MLC phosphorylation fell to lower levels in SA (~28%) than in FA (~42%; see Figs 7B and 8B, for example). This is because the latchbridge model predicts that stress "saturates" at MLC phosphorylation values above ~20% (Hai and Murphy 1988). A decrease in MLC phosphorylation from 40% to 20% causes an increase in the fraction of myosin forming latchbridges (Hai and Murphy 1988). In fact, the signature feature of the latchbridge model is that falling levels of MLC phosphorylation permit high force maintenance at a high energy economy by forming increased numbers of latchbridges (reviewed by (Murphy 1988; Murphy, Rembold et al. 1990)). Thus, the latchbridge model predicts that, at steady-state, SA should contain *more* latchbridges than FA (see Fig 8B). But if this were the case, then based on the knowledge that a higher ratio of latchbridges-to-cycling (phosphorylated) crossbridges would impede crossbridge cycling velocities (Ratz, Hai et al. 1989), force redevelopment at steady-state, a measure of crossbridge cycling velocity (Dillon and Murphy 1982), should be lower in SA than in FA. This was found not to be true. In fact, SA redeveloped force at a much higher rate than did FA (see Fig 9), which is consistent with a report by Eddinger and colleagues that single smooth muscle cells isolated from SA shorten more rapidy than those isolated from FA (Sherwood

and Eddinger 2002). In short, the hypothesis that the motor protein isoforms of SA formed latchbridges is not supported by our data showing that steady-state force fell nearly by half over a 5 min period from initiation of a KCl stimulus, and that SA displayed much higher apparent crossbridge cycling rates despite much lower levels of MLC phosphorylation than FA.

The lower levels of MLC phosphorylation produced by SA compared to FA could not be explained by a lower level of $[Ca^{2+}]_i$ (see Fig 2D). Also, our data using inhibitors of MLC kinase and ROK suggest that additional MLC phosphorylation regulatory systems need not be invoked to explain the differential MLC phosphorylation values comparing FA and SA. Smooth muscle MLC phosphatase catalytic subunit is a PP1δ ser/thr protein phosphatase isoform (Ito, Nakano et al. 2004), and SA expressed nearly 2-fold more PP1 than did FA. Moreover, SA expressed ~20% more MYPT1, the regulatory subunit of MLC phosphatase. Thus, one possible scenario is that because of higher cellular levels of MLC phosphatase in SA compared to FA, the MLC phosphatase-to-kinase ratio was likewise elevated, reducing the steady-state level of MLC phosphorylation for a given $[Ca^{2+}]_i$. This hypothesis is supported by data obtained in permeabilized, Ca^{2+}-clamped tissues, suggesting that MLC phosphatase activity was ~2-fold greater in SA compared to FA.

There has been a great deal of speculation about the function of different MHC and MLC_{17} isoforms (reviewed by (Arner, Lofgren et al. 2003; Morano 2003; Ogut and

Brozovich 2003)). In short, the current thought is that smooth muscles that display the phasic phenotype also display higher relative expression of "faster" myosin isoforms (i.e., SMB and MLC_{17a} compared to SMA and MLC_{17b}; reviewed by (Arner, Lofgren et al. 2003)). Results from the present study support this hypothesis, and provide evidence that the latch-state is not supported by motor proteins expressed by the phasic phenotype. It is interesting that the phasic SA, a branch artery of the FA, displayed such a dramatically different motor protein genotype than its "parent" artery (see Fig 10 and (Sherwood and Eddinger 2002)), but did not display as dramatic a difference in overall genotypic protein expression as did the detrusor compared to FA. However, both the phasic SA and phasic visceral smooth muscles appear to display nearly identical motor protein isoform expression. In conclusion, our data support a model whereby phasic smooth muscle behavior requires an absence of "slow" motor proteins, and therefore, an absence of latchbridge formation, and an absence of stimulus-induced increases in actin polymerization that could strengthen the tonic-phase of contraction. However, our data also support the notion that not all phasic smooth muscle contractions are regulated by identical signaling systems, and that FA and SA contractions are likely regulated by more similar mechanisms than FA and detrusor.

List of References

List of References

Albrecht, K., A. Schneider, et al. (1997). "Exogenous caldesmon promotes relaxation of guinea-pig skinned taenia coli smooth muscles: inhibition of cooperative reattachment of latch bridges?" Pflugers Arch **434**(5): 534-42.

Arner, A., M. Lofgren, et al. (2003). "Smooth, slow and smart muscle motors." J Muscle Res Cell Motil **24**(2-3): 165-73.

Asano, M. and Y. Nomura (2003). "Comparison of inhibitory effects of Y-27632, a Rho kinase inhibitor, in strips of small and large mesenteric arteries from spontaneously hypertensive and normotensive Wistar-Kyoto rats." Hypertens Res **26**(1): 97-106.

Baker, J. E., C. Brosseau, et al. (2003). "The unique properties of tonic smooth muscle emerge from intrinsic as well as intermolecular behaviors of Myosin molecules." J Biol Chem **278**(31): 28533-9.

Battistella-Patterson, A. S., S. Wang, et al. (1997). "Effect of disruption of the cytoskeleton on smooth muscle contraction." Can J Physiol Pharmacol **75**(12): 1287-99.

Bitar, K. N. (2002). "HSP27 phosphorylation and interaction with actin-myosin in smooth muscle contraction." Am J Physiol Gastrointest Liver Physiol **282**(5): G894-903.

Butler, T. M., S. U. Mooers, et al. (1998). "Regulation of catch muscle by twitchin phosphorylation: effects on force, ATPase, and shortening." Biophys J **75**(4): 1904-14.

Butler, T. M., M. J. Siegman, et al. (1986). "Slowing of cross-bridge cycling in smooth muscle without evidence of an internal load." Am J Physiol **251**(6 Pt 1): C945-50.

Conibear, P. B. (1999). "Kinetic studies on the effects of ADP and ionic strength on the interaction between myosin subfragment-1 and actin: implications for load-sensitivity and regulation of the crossbridge cycle." J Muscle Res Cell Motil **20**(8): 727-42.

Cooper, J. A. (1987). "Effects of cytochalasin and phalloidin on actin." J Cell Biol **105**(4): 1473-8.

Dillon, P. F., M. O. Aksoy, et al. (1981). "Myosin phosphorylation and the cross-bridge cycle in arterial smooth muscle." Science **211**(4481): 495-7.

Dillon, P. F. and R. A. Murphy (1982). "High force development and crossbridge attachment in smooth muscle from swine carotid arteries." Circ Res **50**(6): 799-804.

Earley, J. J., X. Su, et al. (1998). "Caldesmon inhibits active crossbridges in unstimulated vascular smooth muscle: an antisense oligodeoxynucleotide approach." Circ Res **83**: 661-667.

Eddinger, T. J. and D. P. Meer (2001). "Single rabbit stomach smooth muscle cell myosin heavy chain SMB expression and shortening velocity." Am J Physiol Cell Physiol **280**(2): C309-16.

Eddinger, T. J. and J. A. Wolf (1993). "Expression of four myosin heavy chain isoforms with development in mouse uterus." Cell Motil Cytoskeleton **25**(4): 358-68.

Eto, M., S. Senba, et al. (1997). "Molecular cloning of a novel phosphorylation-dependent inhibitory protein of protein phosphatase-1 (CPI17) in smooth muscle: its specific localization in smooth muscle." FEBS Lett **410**(2-3): 356-60.

Flavahan, N. A., S. R. Bailey, et al. (2005). "Imaging remodeling of the actin cytoskeleton in vascular smooth muscle cells after mechanosensitive arteriolar constriction." Am J Physiol Heart Circ Physiol **288**(2): H660-9.

Fuglsang, A., A. Khromov, et al. (1993). "Flash photolysis studies of relaxation and cross-bridge detachment: higher sensitivity of tonic than phasic smooth muscle to MgADP." J Muscle Res Cell Motil **14**(6): 666-77.

Gaylinn, B. D., T. J. Eddinger, et al. (1989). "Expression of nonmuscle myosin heavy and light chains in smooth muscle." Am J Physiol **257**(5 Pt 1): C997-1004.

Gerthoffer, W. T. and S. J. Gunst (2001). "Invited review: focal adhesion and small heat shock proteins in the regulation of actin remodeling and contractility in smooth muscle." J Appl Physiol **91**(2): 963-72.

Giulian, G. G., R. L. Moss, et al. (1983). "Improved methodology for analysis and quantitation of proteins on one-dimensional silver-stained slab gels." Anal Biochem **129**(2): 277-87.

Gollub, J., C. R. Cremo, et al. (1999). "Phosphorylation regulates the ADP-induced rotation of the light chain domain of smooth muscle myosin." Biochemistry **38**(31): 10107-18.

Gong, M. C., P. Cohen, et al. (1992). "Myosin light chain phosphatase activities and the effects of phosphatase inhibitors in tonic and phasic smooth muscle." J Biol Chem **267**(21): 14662-8.

Gong, M. C., A. Fuglsang, et al. (1992). "Arachidonic acid inhibits myosin light chain phosphatase and sensitizes smooth muscle to calcium." J Biol Chem **267**: 21492-21498.

Grynkiewicz, G., M. Poenie, et al. (1985). "A new generation of Ca^{2+} indicators with greatly improved fluorescence properties." J Biol Chem **260**: 3440-3450.

Haeberle, J. R. (1994). "Calponin decreases the rate of cross-bridge cycling and increases maximum force production by smooth muscle myosin in an in vitro motility assay." J Biol Chem **269**(17): 12424-31.

Hai, C. M. and H. R. Kim (2004). "An Expanded Latchbridge Model of Protein Kinase C-Mediated Smooth Muscle Contraction." J Appl Physiol.

Hai, C. M. and R. A. Murphy (1988). "Cross-bridge phosphorylation and regulation of latch state in smooth muscle." Am J Physiol **254**(1 Pt 1): C99-106.

Hai, C. M. and R. A. Murphy (1989). "Ca2+, crossbridge phosphorylation, and contraction." Annu Rev Physiol **51**: 285-98.

Harnett, K. M., W. Cao, et al. (2005). "Signal-transduction pathways that regulate smooth muscle function I. Signal transduction in phasic (esophageal) and tonic (gastroesophageal sphincter) smooth muscles." Am J Physiol Gastrointest Liver Physiol **288**(3): G407-16.

Herlihy, J. T. and R. A. Murphy (1973). "Length-tension relationship of smooth muscle of the hog carotid artery." Circ Res **33**: 257-283.

Hewett, T. E., A. F. Martin, et al. (1993). "Correlations between myosin heavy chain isoforms and mechanical parameters in rat myometrium." J Physiol **460**: 351-64.

Himpens, B., G. Matthijs, et al. (1988). "Cytoplasmic free calcium, myosin light chain phosphorylation, and force in phasic and tonic smooth muscle." Journal of General Physiology **92**(6): 713-29.

Himpens, B. and A. P. Somlyo (1988). "Free-calcium and force transients during depolarization and pharmacomechanical coupling in guinea-pig smooth muscle." Journal of Physiology **395**: 507-30.

Horiuti, K., A. V. Somlyo, et al. (1989). "Kinetics of contraction initiated by flash photolysis of caged adenosine triphosphate in tonic and phasic smooth muscles." J Gen Physiol **94**(4): 769-81.

Huang, J., H. Zhou, et al. (2005). "Signaling pathways mediating gastrointestinal smooth muscle contraction and MLC20 phosphorylation by motilin receptors." Am J Physiol Gastrointest Liver Physiol **288**(1): G23-31.

Ito, M., R. Dabrowska, et al. (1989). "Identification in turkey gizzard of an acidic protein related to the C-terminal portion of smooth muscle myosin light chain kinase." J Biol Chem **264**(24): 13971-4.

Ito, M., T. Nakano, et al. (2004). "Myosin phosphatase: structure, regulation and function." Mol Cell Biochem **259**(1-2): 197-209.

Karagiannis, P., G. J. Babu, et al. (2003). "The smooth muscle myosin seven amino acid heavy chain insert's kinetic role in the crossbridge cycle for mouse bladder." J Physiol **547**(Pt 2): 463-73.

Kelley, C. A., M. Takahashi, et al. (1993). "An insert of seven amino acids confers functional differences between smooth muscle myosins from the intestines and vasculature." J Biol Chem **268**(17): 12848-54.

Kenney, R. E., P. E. Hoar, et al. (1990). "The relationship between ATPase activity, isometric force, and myosin light-chain phosphorylation and thiophosphorylation in skinned smooth muscle fiber bundles from chicken gizzard." J Biol Chem **265**(15): 8642-9.

Khromov, A. D., A. V. Somlyo, et al. (1995). "The role of MgADP in force maintenance by dephosphorylated cross-bridges in smooth muscle: a flash photolysis study." Biophys J **69**: 2611-2622.

Kitazawa, T., M. Eto, et al. (2003). "Phosphorylation of the myosin phosphatase targeting subunit and CPI-17 during Ca(2+) sensitization in rabbit smooth muscle." J Physiol **546**(Pt 3): 879-89.

Lamounier-Zepter, V., L. G. Baltas, et al. (2003). "Distinct contractile systems for electromechanical and pharmacomechanical coupling in smooth muscle." Adv Exp Med Biol **538**: 417-25; discussion 425-6.

Lauzon, A. M., M. J. Tyska, et al. (1998). "A 7-amino-acid insert in the heavy chain nucleotide binding loop alters the kinetics of smooth muscle myosin in the laser trap." J Muscle Res Cell Motil **19**(8): 825-37.

Lee, M. R., L. Li, et al. (1997). "Cyclic GMP causes Ca2+ desensitization in vascular smooth muscleby activating the myosin light chain phosphatase." J Biol Chem **272**: 5063-5068.

Lee, Y. H., C. Gallant, et al. (2000). "Regulation of vascular smooth muscle tone by N-terminal region of caldesmon. Possible role of tethering actin to myosin." J Biol Chem **275**(5): 3213-20.

Lofgren, M., E. Ekblad, et al. (2003). "Nonmuscle Myosin motor of smooth muscle." J Gen Physiol **121**(4): 301-10.

Lynn, J. A., J. H. Martin, et al. (1966). "Recent improvements of histologic technics for the combined light and electron microscopic examination of surgical specimens." Am J Clin Pathol **45**(6): 704-13.

Malmqvist, U., K. M. Trybus, et al. (1997). "Slow cycling of unphosphorylated myosin is inhibited by calponin, thus keeping smooth muscle relaxed." Proc Natl Acad Sci U S A **94**(14): 7655-60.

Marston, S., K. Pinter, et al. (1992). "Caldesmon binds to smooth muscle myosin and myosin rod and crosslinks thick filaments to actin filaments." J Muscle Res Cell Motil **13**(2): 206-18.

Masuo, M., S. Reardon, et al. (1994). "A novel mechanism for the Ca(2+)-sensitizing effect of protein kinase C on vascular smooth muscle: inhibition of myosin light chain phosphatase." J Gen Physiol **104**(2): 265-86.

Matthew, J. D., A. S. Khromov, et al. (1998). "Myosin essential light chain isoforms modulate the velocity of shortening propelled by nonphosphorylated cross-bridges." J Biol Chem **273**(47): 31289-96.

Meeks, M. K., M. L. Ripley, et al. (2005). "Heat shock protein 20-mediated force suppression in forskolin-relaxed swine carotid artery." Am J Physiol Cell Physiol **288**(3): C633-9.

Meer, D. P. and T. J. Eddinger (1997). "Expression of smooth muscle myosin heavy chains and unloaded shortening in single smooth muscle cells." Am J Physiol **273**(4 Pt 1): C1259-66.

Mehta, D. and S. J. Gunst (1999). "Actin polymerization stimulated by contractile activation regulates force development in canine tracheal smooth muscle." J Physiol **519 Pt 3**: 829-40.

Mijailovich, S. M., J. P. Butler, et al. (2000). "Perturbed equilibria of myosin binding in airway smooth muscle: bond-length distributions, mechanics, and ATP metabolism." Biophys J **79**(5): 2667-81.

Mitsui, T., T. Kitazawa, et al. (1994). "Correlation between high temperature dependence of smooth muscle myosin light chain phosphatase activity and muscle relaxation rate." J Biol Chem **269**(8): 5842-8.

Morano, I. (2003). "Tuning smooth muscle contraction by molecular motors." J Mol Med **81**(8): 481-7.

Morano, I., G. X. Chai, et al. (2000). "Smooth-muscle contraction without smooth-muscle myosin." Nat Cell Biol **2**(6): 371-5.

Murphy, R. (1988). "Muscle Cells of Hollow Organs." News Physiol Sci **3**(3): 124-128.

Murphy, R. A. (1994). "What is special about smooth muscle? The significance of covalent crossbridge regulation." FASEB J **8**: 311-318.

Murphy, R. A., C. M. Rembold, et al. (1990). "Contraction in smooth muscle: what is latch?" Prog Clin Biol Res **327**: 39-50.

Obara, K., P. T. Szymanski, et al. (1996). "Effects of calponin on isometric force and shortening velocity in permeabilized taenia coli smooth muscle." Am. J. Physiol. **270**: C481-C487.

Ogut, O. and F. V. Brozovich (2003). "Regulation of force in vascular smooth muscle." J Mol Cell Cardiol **35**(4): 347-55.

Ozaki, H. and H. Karaki (1993). "Different Ca(2+)-sensitivity in phasic and tonic types of smooth muscles." Biol Signals **2**(5): 253-62.

Patton, C., S. Thompson, et al. (2004). "Some precaustions in using chelators to buffer metals in biological solutions." Cell Calcium **35**(5): 427-31.

Paul, R. J. (1990). "Smooth muscle energetics and theories of cross-bridge regulation." Am J Physiol **258**(2 Pt 1): C369-75.

Paul, R. J., G. E. Shull, et al. (2002). "The sarcoplasmic reticulum and smooth muscle function: evidence from transgenic mice." Novartis Found Symp **246**: 228-38; discussion 238-43, 272-6.

Rasmussen, H., Y. Takuwa, et al. (1987). "Protein kinase C in the regulation of smooth muscle contraction." Faseb J **1**(3): 177-85.

Ratz, P. H. (1993). "High α_1-adrenergic receptor occupancy decreases relaxing potency of nifedipine by increasing myosin light chain phosphorylation." Circ Res **72**: 1308-1316.

Ratz, P. H., K. M. Berg, et al. (2005). "Regulation of smooth muscle calcium sensitivity: KCl as a calcium-sensitizing stimulus." Am J Physiol Cell Physiol **288**(4): C769-83.

Ratz, P. H., C.-M. Hai, et al. (1989). "Dependence of stress on cross-bridge phosphorylation in vascular smooth muscle." Am J Physiol **256**: C96-C100.

Ratz, P. H., J. T. Meehl, et al. (2002). "RhoA kinase and protein kinase C participate in regulation of rabbit stomach fundus smooth muscle contraction." Br J Pharmacol **137**(7): 983-92.

Ratz, P. H. and R. A. Murphy (1987). "Contributions of intracellular and extracellular Ca^{2+} pools to activation of myosin phosphorylation and stress in swine carotid media." Circ Res **60**: 410-421.

Rembold, C. M. and R. A. Murphy (1990). "Latch-bridge model in smooth muscle: [Ca2+]i can quantitatively predict stress." Am J Physiol **259**(2 Pt 1): C251-7.

Rhee, A. Y. and F. V. Brozovich (2003). "Force maintenance in smooth muscle: analysis using sinusoidal perturbations." Arch Biochem Biophys **410**(1): 25-38.

Rovner, A. S., Y. Freyzon, et al. (1997). "An insert in the motor domain determines the functional properties of expressed smooth muscle myosin isoforms." J Muscle Res Cell Motil **18**(1): 103-10.

Sherwood, J. J. and T. J. Eddinger (2002). "Shortening velocity and myosin heavy- and light-chain isoform mRNA in rabbit arterial smooth muscle cells." Am J Physiol Cell Physiol **282**(5): C1093-102.

Somlyo, A. P. and A. V. Somlyo (1968). "Vascular smooth muscle. I. Normal structure, pathology, biochemistry, and biophysics." Pharmacol Rev **20**(4): 197-272.

Somlyo, A. P. and A. V. Somlyo (2003). "Ca2+ sensitivity of smooth muscle and nonmuscle myosin II: modulated by G proteins, kinases, and myosin phosphatase." Physiol Rev **83**(4): 1325-58.

Somlyo, A. V., J. D. Matthew, et al. (1998). "Regulation of the cross-bridge cycle: the effects of MgADP, LC17 isoforms and telokin." Acta Physiol Scand **164**(4): 381-8.

Somlyo, A. V. and A. P. Somlyo (1968). "Electromechanical and pharmacomechanical coupling in vascular smooth muscle." J Pharmacol Exp Ther **159**(1): 129-145.

Sutherland, C. and M. P. Walsh (1989). "Phosphorylation of caldesmon prevents its interaction with smooth muscle myosin." J Biol Chem **264**(1): 578-83.

Szymanski, P. T. (2004). "Calponin (CaP) as a latch-bridge protein--a new concept in regulation of contractility in smooth muscles." J Muscle Res Cell Motil **25**(1): 7-19.

Szymanski, P. T., T. K. Chacko, et al. (1998). "Differences in contractile protein content and isoforms in phasic and tonic smooth muscles." Am J Physiol **275**(3 Pt 1): C684-92.

Trybus, K. M. (1991). "Regulation of smooth muscle myosin." Cell Motil Cytoskeleton **18**(2): 81-5.

Urban, N. H., K. M. Berg, et al. (2003). "K+ depolarization induces RhoA kinase translocation to caveolae and Ca2+ sensitization of arterial muscle." Am J Physiol Cell Physiol **285**(6): C1377-85.

Walsh, M. P. and C. Sutherland (1989). "A model for caldesmon in latch-bridge formation in smooth muscle." Adv Exp Med Biol **255**: 337-46.

Weber, L. P., M. Seto, et al. (2000). "The involvement of protein kinase C in myosin phosphorylation and force development in rat tail arterial smooth muscle." Biochem J **352 Pt 2**: 573-82.

Woodsome, T. P., M. Eto, et al. (2001). "Expression of CPI-17 and myosin phosphatase correlates with Ca^{2+} sensitivity of protein kinase C-induced contraction in rabbit smooth muscle." J Physiol **535**: 553-564.

Wright, G. and E. Hurn (1994). "Cytochalasin inhibition of slow tension increase in rat aortic rings." Am J Physiol **267**(4 Pt 2): H1437-46.

Yan, B., A. Sen, et al. (2003). "Theoretical studies on competitive binding of caldesmon and myosin S1 to actin: prediction of apparent cooperativity in equilibrium and slow-down in kinetics of S1 binding by caldesmon." Biochemistry **42**(14): 4208-16.

Yu, S. N., P. E. Crago, et al. (1997). "A nonisometric kinetic model for smooth muscle." Am J Physiol **272**(3 Pt 1): C1025-39.

VITA

Shaojie Han was born on February 18, 1973 in Wuhan, China to Weizhong Han and Sue Xu. He received his Bachelor of Medicine in 1995 and Master of Medicine in 2002 from Tongji Medical College, China. From 1995 to 1999, he worked as a physician and did clinic research in China.